
Masters Theses


Student Theses and Dissertations

Fall 2015

Healing of bone defects in a rodent calvarial defect model using strong porous bioactive glass (13-93) scaffolds

Yinan Lin

Follow this and additional works at: https://scholarsmine.mst.edu/masters_theses

 Part of the [Biology Commons](#), [Biomedical Engineering and Bioengineering Commons](#), and the [Materials Science and Engineering Commons](#)

Department:

Recommended Citation

Lin, Yinan, "Healing of bone defects in a rodent calvarial defect model using strong porous bioactive glass (13-93) scaffolds" (2015). *Masters Theses*. 7470.

https://scholarsmine.mst.edu/masters_theses/7470

This thesis is brought to you by Scholars' Mine, a service of the Missouri S&T Library and Learning Resources. This work is protected by U. S. Copyright Law. Unauthorized use including reproduction for redistribution requires the permission of the copyright holder. For more information, please contact scholarsmine@mst.edu.

HEALING OF BONE DEFECTS IN A RODENT CALVARIAL DEFECT MODEL
USING STRONG POROUS BIOACTIVE GLASS (13-93) SCAFFOLDS

by

YINAN LIN

A THESIS

Presented to the Faculty of the Graduate School of the

MISSOURI UNIVERSITY OF SCIENCE AND TECHNOLOGY

In Partial Fulfillment of the Requirements for the Degree

MASTER OF SCIENCE

in

MATERIAL SCIENCE AND ENGINEERING

2015

Approved by

Dr. Mohamed N. Rahaman, Advisor
Dr. Richard K. Brow
Dr. Sonny B. Bal

PUBLICATION THESIS OPTION

The body of this thesis has been compiled in the format for publication in peer-reviewed journals. Two papers have been included in the following order.

The first paper, pages 2-40, “Long-term Bone Regeneration, Mineralization and Angiogenesis in Rat Calvarial Defects Implanted with Strong Porous Bioactive Glass (13-93) Scaffolds,” was accepted for publication in *Journal of Non-Crystalline Solids* in 2015.

The second paper, pages 41-89, “Response of Osteoblastic MC3T3-E1 Cells and Osseous Defects to Strong Porous Scaffolds of Silicate 13-93 Bioactive Glass Doped with Copper,” was submitted to *Biomedical Glasses*.

ABSTRACT

The main objective of this project was to evaluate the capacity of strong porous silicate (13-93) bioactive glass scaffolds prepared by a robocasting technique to regenerate bone and stimulate angiogenesis in a rat calvarial defect model. The scaffolds were created with the same grid-like microstructure but in a variety of formulations: (i) as-fabricated, (ii) pretreated in an aqueous phosphate solution to convert the glass surface to hydroxyapatite, (iii) loaded with bone morphogenetic protein-2 (BMP2) (1 μg per scaffold), and (iv) doped with copper (0.4–2.0 wt. % CuO). When compared to the as-fabricated scaffolds, the pretreated scaffolds enhanced bone regeneration at 6 weeks but not at 12 or 24 weeks. In comparison, the BMP2-loaded scaffolds enhanced bone regeneration at all three implantation times and they were almost completely infiltrated with lamellar bone within 12 weeks. Doping the as-fabricated scaffolds with 0.4 and 0.8 wt. % CuO did not affect the response of preosteoblastic MC3T3-E1 cells in vitro and bone regeneration in vivo. In comparison, the scaffolds doped with 2.0 wt. % CuO were toxic to the cells in vitro and significantly inhibited bone regeneration at 6 weeks post-implantation. The area of new blood vessels in the new bone that infiltrated the scaffolds at 6 weeks post-implantation was significantly enhanced by the BMP2 loading but not by CuO dopant concentrations of 0.4 and 0.8 wt. %. The fibrous tissue that infiltrated the scaffolds doped with 2.0 wt. % CuO showed a significantly higher blood vessel area than the as-fabricated scaffolds. Loading silicate 13-93 bioactive glass scaffolds with BMP2 significantly improved their capacity to regenerate bone in rat calvarial defects at 6 weeks post-implantation when compared to doping the glass with copper.

ACKNOWLEDGEMENTS

I thank my advisor, Dr. Mohamed N. Rahaman, for his guidance during this project. I sincerely appreciate the assistance of Dr. Roger F. Brown with the *in vitro* and *in vivo* experiments. I am also grateful to my thesis advisory committee, Dr. Richard K. Brow, and Dr. B. Sonny Bal, for their valuable comments and constructive suggestions.

All of my friends and colleagues deserve many thanks as well. Working and learning with you brought a great deal of joy to my life. Many thanks to Wei Xiao, Youqu Shen, Sixie Huang and others. My research would not have been possible without their help.

Last but not the least, I cannot say enough about the support I have received from both my parents, Hui Lin and Weihua Liu, and my wife, Lina Ma. They were always there cheering me up and stood by me in both good times and bad supporting me and encouraging me with their best wishes. I would not have been able to complete this thesis without them.

TABLE OF CONTENTS

	Page
PUBLICATION THESIS OPTION.....	iii
ABSTRACT.....	iv
ACKNOWLEDGMENTS	v
LIST OF ILLUSTRATIONS.....	ix
LIST OF TABLES	xii
SECTION	
1. PURPOSE OF THIS THESIS	1
PAPER	
I. Long-term bone regeneration, mineralization and angiogenesis in rat calvarial defects implanted with strong porous bioactive glass (13-93) scaffolds.....	2
ABSTRACT	2
1. Introduction	4
2. Materials and methods.....	6
2.1 Preparation of scaffolds	6
2.2 Animals and surgical procedure.....	7
2.3 Histologic processing.....	9
2.4 Histomorphometric analysis	9
2.5 Scanning electron microscopy	11
2.6 Statistical analysis	11
3. Results	11
3.1 Assessment of bone regeneration.....	12
3.2 Assessment of bone marrow and fibrous tissue.....	14
3.3 Assessment of mineralized tissue and bioactive glass conversion	14
3.4. SEM evaluation of implants.....	16
3.5 Assessment of angiogenesis.....	17
4. Discussion.....	19
5. Conclusions	24

Acknowledgements	25
References	25
II. Response of osteoblastic MC3T3-E1 cells and osseous defects to strong porous scaffolds of silicate 13-93 glass doped with copper	39
ABSTRACT	39
1.Introduction	40
2.Materials and methods.....	43
2.1 Preparation of scaffolds	43
2.2 Degradation and conversion of scaffolds in simulated body fluid (SBF)	45
2.3 Cell culture	46
2.3.1 Cell morphology	46
2.3.2 Cell viability and proliferation.....	47
2.3.3 Alkaline phosphatase (ALP) activity	48
2.4. Evaluation of scaffolds in rat calvarial defects in vivo	49
2.4.1 Animals and surgical procedure.....	49
2.4.2 Histologic processing	50
2.4.3 Histomorphometric analysis	51
2.5 Statistical analysis	52
3. Results	52
3.1 Characteristics of as-fabricated scaffolds	52
3.2 Degradation and conversion of scaffolds to hydroxyapatite in SBF	53
3.3 Assessment of MC3T3-E1 cell proliferation and ALP activity in vitro	54
3.4 Assessment of new bone formation in rat calvarial defects in-vivo	56
3.5 Assessment of mineralized tissue and bioactive glass conversion	57
3.6 Assessment of fibrous tissue and marrow-like tissue	58
3.7 Assessment of angiogenesis.....	58
4. Discussion.....	59
4.1 Release of Cu ions from scaffolds into SBF in vitro	60
4.2 Effect of Cu-doped scaffolds on MC3T3-E1 cell proliferation and function .	61
4.3 Effect of Cu-doped scaffolds on bone regeneration and angiogenesis	64
5. Conclusion.....	67

References 67

SECTION

 2. CONCLUSIONS..... 86

VITA.....88

LIST OF ILLUSTRATIONS

PAPER I	Page
Fig. 1. Optical image of 13-93 bioactive glass scaffold prepared by robocasting for implantation in rat calvarial defects. Higher-magnification SEM image of the scaffold showing dense glass filaments and porous grid-like architecture in the plane of deposition.	29
Fig. 2. Transmitted light images of H&E-stained sections of rat calvarial defects implanted for 6 weeks, 12 weeks and 24 weeks with the three groups of bioactive glass scaffolds: as-fabricated, pretreated and BMP2-loaded. Higher magnification images of the boxed areas in c1–c3 are shown in d1–d3. N = new bone; O = host bone; * = bony island; G = bioactive glass; arrowheads indicate the edges of host bone.....	30
Fig. 3. Percent new bone in rat calvarial defects implanted with the three groups of scaffolds for 6, 12 and 24 weeks. The amount of new bone is shown as a percent of the available pore space of the scaffolds.	31
Fig. 4. Percent bone marrow-like tissue and fibrous tissue in rate calvarial defects implanted with the three groups of scaffolds for 6, 12 and 24 weeks.	32
Fig. 5. Transmitted light images of von Kossa stained sections of rat calvarial defects implanted for 6 weeks, 12 weeks and 24 weeks with the three groups of bioactive glass scaffolds: as-fabricated, pretreated and BMP2-loaded. N = new bone; O = host bone; G = bioactive glass; arrowheads indicate the edges of host bone.	33
Fig. 6. Percent total von Kossa positive area and vK+ area due to the bioactive glass conversion, determined as a fraction of the total defect area, for rat calvarial defects implanted with the three groups of scaffolds at 6, 12 and 24 weeks post-implantation.	34
Fig. 7. Backscattered SEM images of rat calvarial defects implanted with bioactive glass scaffolds at 24 weeks post-implantation: as-fabricated scaffolds; pretreated scaffolds; BMP2-loaded. N = new bone; G = bioactive glass. The approximate thickness of the converted surface layer on the glass filaments are shown in a2 – c2.	35
Fig. 8. Transmitted light images of PAS stained sections of rat calvarial defects implanted with the three groups of bioactive glass scaffolds at 12 weeks post-implantation: as-fabricated scaffolds; pretreated scaffolds; BMP2-loaded scaffolds.....	36

Fig. 9. Percent blood vessel area and number of blood vessels per unit area of new bone in rat calvarial defects implanted with the three groups of scaffolds at 6, 12 and 24 weeks post-implantation.	37
---	----

PAPER II

Fig. 1. Optical image of the four groups of as-fabricated scaffolds prepared by robocasting, composed of 13-93 glass and 13-93 glass doped with 0.4, 0.8 and 2.0 wt. % CuO; SEM image of the top surface of a 13-93 scaffold doped with 0.8 wt. % CuO; SEM image of the surface of a glass filament after immersion of the scaffold in SBF at 37 °C for 7 days.....	72
Fig. 2. Weight loss of 13-93 scaffolds and scaffolds doped with 0.4, 0.8 and 2.0 wt. % CuO and cumulative amount of Cu ions released from 13-93 scaffolds doped with 0.4, 0.8 and 2.0 wt. % CuO as a function of immersion time in SBF. ..	73
Fig. 3. Cell proliferation, as measured by CCK-8 assay, of MC3T3-E1 cells cultured on the four groups of bioactive glass scaffolds for the times shown.....	74
Fig. 4. Fluorescent images of MC3T3-E1 cells incubated for 2, 7, 14 and 21 days on the four groups of bioactive glass scaffolds. Double staining was used to detect live cells as green fluorescent and dead cells as red fluorescent.	75
Fig. 5. SEM images of the four groups of bioactive glass scaffolds seeded with MC3T3-E1 cells and incubated for 2, 7 and 14 days.	76
Fig. 6. Alkaline phosphatase activity of MC3T3-E1 cells cultured on 13-93 scaffolds and on 13-93 scaffolds doped with 0.4, 0.8 and 2.0 wt. % CuO for the times shown. Enzyme activity is expressed as ng of pNP formed per μ g dsDNA per 30 min.....	77
Fig. 7. Transmitted light images of H&E-stained sections of rat calvarial defects implanted with the four groups of bioactive glass scaffolds, as fabricated or loaded with BMP2, at 6 weeks postimplantation.	78
Fig. 8. Percent new bone in rat calvarial defects implanted with the four groups of scaffolds, 13-93 and 13-93 doped with 0.4, 0.8 and 2.0 wt. % CuO, as-fabricated or loaded with BMP2, at 6 weeks postimplantation. The amount of new bone is shown as a percent of the available pore space of the scaffolds.	79
Fig. 9. Transmitted light images of von Kossa stained sections of rat calvarial defects implanted with the four groups of scaffolds, as-fabricated or loaded with BMP2, at 6 weeks postimplantation.....	80
Fig. 10. Percent total von Kossa positive area and vK+ area due to the bioactive glass conversion, determined as a fraction of the total defect area, for rat calvarial defects implanted with the four groups of scaffolds, as fabricated or loaded with BMP2, at 6 weeks post-implantation.....	81

- Fig. 11. Percent bone marrow-like tissue and fibrous tissue in rat calvarial defects implanted with the four groups of scaffolds, as fabricated or loaded with BMP2, at 6 weeks post-implantation.....82
- Fig. 12. Transmitted light images of PAS stained sections of rat calvarial defects implanted with the four groups of scaffolds at 6 weeks postimplantation; magnified images of the boxed areas in the corresponding images on the left.83
- Fig. 13. Percent blood vessel area in rat calvarial defects implanted with the four groups of scaffolds at 6 weeks postimplantation. The blood vessel area in the fibrous tissue and in the new bone are shown as a percentage of the total fibrous tissue and total new bone, respectively.84
- Fig. S1. Raman spectra of the un-doped 13-93 scaffold and the 13-93 bioactive glass scaffolds doped with 0.4 wt.% CuO, 0.8 wt.% CuO and 2 wt.% CuO after immersion in SBF for 28 days.....85

LIST OF TABLES

PAPER I

Table I. Calcium to phosphorus atomic ratio for new bone, converted glass layer, silica-rich layer and unconverted glass in rat calvarial defects implanted with as-fabricated, pretreated and BMP2-loaded scaffolds at 12 and 24 weeks post-implantation.....	38
--	----

1. PURPOSE OF THIS THESIS

The main purpose of this research was to create and evaluate strong porous 13-93 scaffolds of bioactive glass with grid-like architectures for potential applications in loaded bone repair.

Bioactive glass and ceramics have been widely investigated for healing bone defects, because of their ability to enhance bone formation and to bond with surrounding tissue. The glass designated 13-93 (53 SiO₂, 6 Na₂O, 12 K₂O; 5 MgO, 20 CaO and 4 P₂O₅, wt%) is a silicate-based bioactive glass with a modified 45S5 composition, which has better processing characteristics by viscous flow sintering than the 45S5 bioactive glass. When fabricated into 3D scaffolds, the 13-93 bioactive glass can be sintered to high density without crystallization, which leads to optimum scaffold strength. Previous research in our research group (Xin et al) showed that the 13-93 bioactive scaffolds with a grid-like microstructure, prepared by a robocasting technique, had higher mechanical properties than scaffolds prepared by more conventional methods, such as the polymer foam replication technique, which make them potential candidates for loaded bone repair.

In this work, the grid-like 13-93 bioactive glass scaffolds were fabricated by a robocasting method and their ability to support bone regeneration and angiogenesis were evaluated in osseous defects over a long-term duration. The ability to support bone regeneration of the scaffolds doped with various amount of CuO were studied and compared with un-doped 13-93 scaffolds.

PAPER

I. Long-term bone regeneration, mineralization and angiogenesis in rat calvarial defects implanted with strong porous bioactive glass (13-93) scaffolds

Yinan Lin¹, Wei Xiao¹, Xin Liu¹, B. Sonny Bal², Lynda F. Bonewald³, Mohamed N. Rahaman^{1,*}

¹Department of Materials Science and Engineering Missouri University of Science and Technology, Rolla, MO 65409, USA

²Department of Orthopaedic Surgery, School of Medicine, University of Missouri–Columbia, MO 65212, USA

³Department of Oral and Craniofacial Sciences, School of Dentistry, University of Missouri– Kansas City, Kansas City, MO 64108, USA

ABSTRACT

There is growing interest in the use of bioactive glass scaffolds for repairing structural bone defects but data on the capacity of the scaffolds to regenerate bone *in vivo*, particularly over a long-term duration, are limited. In this study, bone regeneration in rat calvarial defects implanted with strong porous scaffolds of silicate 13-93 glass (porosity = $47 \pm 1\%$) was investigated at 12 and 24 weeks post-implantation and compared with previous results from a similar study at 6 weeks. Three groups of implants, composed of as-fabricated scaffolds, scaffolds pretreated in a phosphate solution to convert a thin surface layer (5 μm) to hydroxyapatite (HA) and pretreated scaffolds loaded with bone morphogenetic protein-2 (BMP2) (1 $\mu\text{g}/\text{defect}$) were used. Bone regeneration, bioactive glass conversion to HA and blood vessel formation in the defects implanted with the three groups of scaffolds were evaluated using histology, histomorphometric analysis and scanning electron microscopy. When compared to the as-fabricated scaffolds, the

pretreated scaffolds enhanced bone regeneration at 6 weeks but not at 12 or 24 weeks. In comparison, the BMP2-loaded scaffolds showed a significantly better capacity to regenerate bone at all three implantation times and they were almost completely infiltrated with lamellar bone within 12 weeks. The amount of glass conversion to HA at 24 weeks (30–33%) was not significantly different among the three groups of scaffolds. The area and number of blood vessels in the new bone that infiltrated the BMP2-loaded scaffolds at 6 and 12 weeks post-implantation were significantly greater than those for the as-fabricated and pretreated scaffolds. However, there was no significant difference in blood vessel area and number among the three groups of scaffolds at 24 weeks. The results indicate that these strong porous bioactive glass (13-93) scaffolds loaded with BMP2 are promising candidate implants for structural bone repair.

1. Introduction

There is growing interest in the development of bioactive glass scaffolds for healing large (critical size) bone defects, particularly defects in structural bone. The attractive properties of bioactive glasses as a scaffold material for bone repair, such as their ability to stimulate osteogenesis, convert to hydroxyapatite (HA) (the mineral constituent of bone) and bond strongly to bone, have been well documented for 30–40 years [1–4]. However, most previous studies have targeted bioactive glass in the form of particles, granules or low strength porous scaffolds that have inadequate mechanical properties for structural bone repair [5]. Furthermore, while several investigations have been performed to study the capacity of bioactive glass scaffolds to regenerate bone in osseous defects *in vivo*, the available data covering longer-term implantation times, such as times longer than 6–12 weeks, are limited.

Recent studies have shown the ability to create strong porous scaffolds of silicate 13-93 or 6P53B bioactive glass by robotic deposition techniques such as freeze extrusion fabrication [6] and robocasting [7, 8]. Scaffolds with a grid-like microstructure (porosity ~50%; pore width ~300 μm) showed compressive strengths (~140 MPa) that were comparable to human cortical bone (100–150 MPa) [5]. Strong porous scaffolds of 13-93 glass created by robocasting also showed excellent fatigue resistance *in vitro* under compressive stresses that were higher than normal physiologic stresses on the femur of humans [9].

When implanted for 6 weeks in rat calvarial defects (4.6 mm in diameter), strong porous scaffolds of 13-93 bioactive glass were infiltrated with new bone and they integrated with host bone [10]. Pretreating the as-fabricated scaffolds in an aqueous

phosphate solution to convert a thin surface layer (~5 μm) of the glass to HA prior to implantation significantly improved their capacity to regenerate bone. Loading the pretreated scaffolds with bone morphogenetic protein-2 (BMP2) (1 $\mu\text{g}/\text{defect}$) prior to implantation further enhanced their capacity to regenerate bone. Approximately 65% of the pore volume of the BMP2-loaded scaffolds was infiltrated with new bone at 6 weeks.

More recent studies have shown promising results for the use of strong porous 13-93 bioactive glass scaffolds in healing structural bone defects in small animals [11]. When implanted for 12 weeks in rat femoral segmental defects (6 mm long) using intramedullary pin fixation, the ends of the 13-93 scaffolds were infiltrated with new bone, resulting in integration. The percent new bone in the defects implanted with the 13-93 scaffolds (25%) was not significantly different from that in the defects implanted with autografts (38%) ($n = 6$; $p < 0.05$). In another study, cylindrical scaffolds of 13-93 glass (porosity = 55–67%; compressive strength = 40 MPa) were prepared by selective laser sintering and evaluated in rat femoral segmental defects (5 mm long) [12]. The scaffolds contained drill holes in the sides of the cylinder that were either filled with dicalcium phosphate dihydrate (DCPD) used as a carrier for BMP2 (10 $\mu\text{g}/\text{defect}$) or left unfilled (control group). X-ray radiography and micro-computed tomography (micro-CT) showed the formation of bridging calluses around both groups of implants but faster healing and better callus formation were found for the BMP2-loaded scaffolds.

In view of the capacity of strong porous bioactive glass (13-93) scaffolds to regenerate bone in rat calvarial defects at 6 weeks and to heal segmental bone defects in rodents at 12 weeks, this study was undertaken to evaluate longer term bone regeneration in osseous defects implanted with those strong porous 13-93 scaffolds. Implantation times

longer than 6–12 weeks are necessary for better evaluating the capacity of the scaffolds to heal the defect, maintain healthy bone growth and convert to HA. Two groups of scaffolds, pretreated for three days in an aqueous phosphate solution or loaded with BMP2, were implanted in rat calvarial defects for 12 and 24 weeks. The as-fabricated scaffolds (no pretreatment or BMP2) were used as the control group. Bone regeneration, glass conversion to HA and blood vessel formation in the defects implanted with the scaffolds were evaluated using histology, histomorphometric analysis and scanning electron microscopy. The results were compared with those obtained in a previous study for similar scaffolds implanted for 6 weeks in the same animal model [10].

2. Materials and methods

2.1 Preparation of scaffolds

Scaffolds with a grid-like microstructure were prepared using a robotic deposition (robocasting) method, as described in detail elsewhere [9, 10]. Briefly, the as-received 13-93 glass (Mo-Sci Corp., Rolla, MO) was ground to form particles ($\sim 1 \mu\text{m}$), mixed with a 20 wt% Pluronic-127 binder solution to form a paste (40 vol% glass particles) and extruded using a robocasting machine (RoboCAD 3.0; 3-D Inks, Stillwater, OK). After drying at room temperature, the scaffolds were heated in O_2 at a rate of $0.5 \text{ }^\circ\text{C}/\text{min}$ to $600 \text{ }^\circ\text{C}$ to burn out the processing additives, and sintered for 1 h at $700 \text{ }^\circ\text{C}$ (heating rate = $5 \text{ }^\circ\text{C}/\text{min}$) to densify the glass filaments. The as-fabricated scaffolds were sectioned and ground to form thin discs (4.6 mm in diameter \times 1.5 mm), washed twice with deionized water and twice with anhydrous ethanol, dried in air and sterilized by heating for 12 h at $250 \text{ }^\circ\text{C}$. For reference, images of the as-fabricated scaffolds are shown in **Fig. 1**.

Twenty-eight of the as-fabricated scaffolds were reacted for 3 days in an aqueous phosphate solution (0.25 M K_2HPO_4 solution) at 60 °C and a starting pH of 12.0 to convert a thin surface layer of the glass to HA (or amorphous calcium phosphate, ACP), as described previously [10]. The mass of the glass scaffolds to the volume of the K_2HPO_4 solution was kept constant at 1 g per 200 ml and the solution was stirred gently each day. Fourteen of the pretreated scaffolds were loaded with BMP2 prior to implantation using a procedure described previously [10]. Briefly, a solution of BMP2 (Shenandoah Biotechnology Inc., PA, USA) in citric acid was prepared by dissolving 10 μ g of BMP2 in 100 μ l sterile citric acid (pH = 3.0). Then 10 μ l of the BMP2 solution was pipetted on to each bioactive glass scaffold. The BMP2 solution was completely absorbed within the converted surface layer of the scaffolds and there was no visible evidence for any of the solution flowing out of the scaffolds. After loading with BMP2, the scaffolds were kept for ~24 h in a refrigerator at 4 °C to dry them prior to implantation. The release profile of the BMP2 from the scaffolds into a solution composed of equal volumes of fetal bovine serum (FBS) and phosphate-buffered saline (PBS) plus 1 vol. % penicillin was measured previously as a function of time *in vitro* [10].

2.2 Animals and surgical procedure

All animal experimental procedures were approved by the Animal Care and Use Committee, Missouri University of Science and Technology, in compliance with the NIH Guide for Care and Use of Laboratory Animals (1985). The three groups of scaffolds (described as as-fabricated, pretreated and BMP2-loaded) were implanted in rat calvarial defects for 12 and 24 weeks. Seven scaffolds from each group were implanted for each

implantation time. This sample size ($n = 7$) was selected on the basis of the results of a previous study for an implantation time of 6 weeks [10] and a power analysis. The implants were assigned randomly to the defects, but scaffolds with and without BMP2 were not mixed in the same animal.

Twenty-two male Sprague Dawley rats (3 months old; weight = 350–400 g, Harlan Laboratories Inc., USA) were maintained in the animal facility for 2 weeks to become acclimated to diet, water and housing. The rats were anesthetized with a combination of ketamine (72 mg/kg) and xylazine (6 mg/kg) and maintained under anesthesia with ether gas in oxygen. The surgical site was shaved, scrubbed with iodine and draped. Using sterile instruments and aseptic technique, a cranial skin incision was sharply made in an anterior to posterior direction along the midline. The subcutaneous tissue, musculature and periosteum were dissected and reflected to expose the calvarium. Bilateral full-thickness defects 4.6 mm in diameter were created in the central area of each parietal bone using a saline-cooled trephine drill. The dura mater was not disturbed. The sites were constantly irrigated with sterile PBS to prevent overheating of the bone margins and to remove the bone debris. After the bilateral defect was implanted with the scaffold, the periosteum and skin were repositioned and closed using wound clips. Post-surgery, the animals were given a dose of ketoprofen (3 mg/kg) intramuscularly and ~200 μ l penicillin subcutaneously. The animals were monitored daily for the condition of the surgical wound, food intake, activity and clinical signs of infection. After 12 and 24 weeks, the animals were sacrificed by CO₂ inhalation, and the calvarial defect sites with surrounding bone and soft tissue were harvested for evaluation.

2.3 Histologic processing

The calvarial samples, including the surgical sites with surrounding bone and tissue, were fixed in 10% buffered formaldehyde for 3 days, then transferred into 70% ethanol and cut in half. Half of each sample was for paraffin embedding and the other half for methyl methacrylate embedding. The samples for paraffin embedding were de-siliconized by immersion for 2 h in 10% hydrofluoric acid, decalcified in 14% ethylenediaminetetraacetic acid (EDTA) for 4 weeks, dehydrated in a series of graded ethanol and embedded in paraffin using routine histological techniques. Then the specimens were sectioned to 5 μm using a microtome and stained with hematoxylin and eosin (H&E) and by the periodic acid-Schiff (PAS) technique. The un-decalcified samples were dehydrated in ethanol and embedded in PMMA. Sections were affixed to acrylic slides, ground down to 40 μm using a surface grinder (EXAKT 400CS, Norderstedt, Germany) and stained using the von Kossa method. Transmitted light images of the stained sections were taken with an Olympus BX 50 microscope connected to a CCD camera (DP70, Olympus, Japan).

2.4 Histomorphometric analysis

Histomorphometric analysis was carried out using optical images of the stained sections and the ImageJ software (National Institutes of Health, USA). One section across the diameter of each defect was analyzed. The percent new bone formed in the defects was evaluated from the H&E stained sections. The entire defect area was determined as the area between the two defect margins, including the entire glass scaffold and the tissue within. The available pore area within the scaffold was determined by subtracting the area of the

bioactive glass scaffold from the total defect area. The newly formed bone, fibrous tissue and bone marrow-like tissue within the defect area were then outlined and measured. The area of each tissue was expressed as a percentage of the available pore area of the scaffolds and total defect area.

The von Kossa-positive area in the defects implanted with the scaffolds was analyzed using the von Kossa stained sections and ImageJ. One section across the diameter of each defect was analyzed. Images were adjusted to measure only the black-stained areas of the image, which yielded the black area fraction as a percentage of the total defect area. As mineralized bone and HA both bound the silver nitrate, in order to determine the percent area due to the conversion of the glass scaffold, the von Kossa-positive percentage was averaged for each sample and the percent new bone determined for each sample from the H&E stained images was subtracted.

Quantitation of blood vessels within the defect was performed using the sections stained by the PAS technique, which results in purple-stained blood vessels with counterstaining yielding green red blood cells. Viewed at 20x field, each scaffold was scanned to acquire six regions of interest within the new bone and the blood vessels were outlined. All six areas were combined using ImageJ to determine the total blood vessel area, which was expressed as a percentage of the area of the selected regions. The total number of blood vessels in the six areas was determined and normalized to unit area (1 mm²) of the new bone.

2.5 Scanning electron microscopy

Unstained sections of the implants in poly(methyl methacrylate) (PMMA) were coated with carbon and examined in a field-emission scanning electron microscope (FESEM) (S-4700; Hitachi, Tokyo, Japan) fitted with an energy-dispersive X-ray (EDS) spectrometer. The specimens were examined at an accelerating voltage of 15 kV and a working distance of 12 mm. The calcium to phosphorus (Ca/P) atomic ratio of the glass converted to HA, new bone and unconverted glass were measured using the as-received glass and a reference HA as standards. The thickness of the converted layer on the filaments of the scaffolds was determined as the average from three randomly selected regions.

2.6 Statistical analysis

The data are presented as a mean \pm standard deviation (SD). Analysis for differences in new bone, mineralized tissue, and blood capillary area and number between groups was performed using one-way analysis of variance (ANOVA) with Tukey's post hoc test. Differences were considered significant for $p < 0.05$.

3. Results

The three groups of 13-93 bioactive glass scaffolds used in this study were similar to those implanted previously for 6 weeks in the same animal model [10]. The as-fabricated scaffold had a grid-like microstructure (**Fig. 1**), composed of almost fully dense 13-93 glass filaments of diameter $330 \pm 10 \mu\text{m}$ and pores of width $300 \pm 10 \mu\text{m}$ in the plane of deposition (xy plane) and $150 \pm 10 \mu\text{m}$ in the direction perpendicular to the deposition plane (z direction). The porosity of the scaffolds was $47 \pm 1\%$, as measured using the Archimedes method. Pretreatment of the as-fabricated scaffolds in an aqueous phosphate

(K₂HPO₄) solution resulted in a porous HA surface layer on the glass filaments of thickness = 5 ± 2 μm and surface area = 30 ± 3 m^2/g .

3.1 Assessment of bone regeneration

Transmitted light images of H&E stained sections of the rat calvarial defects implanted for 12 and 24 weeks with the as-fabricated, pretreated and BMP2-loaded scaffolds are shown in **Fig. 2**. Stained sections of defects implanted for 6 weeks with the three groups of scaffolds, obtained in a previous study [10], are included for comparison. New bone infiltrated all three groups of scaffolds, into the edges (periphery) adjacent to the host bone and into the pores, indicating good integration of the scaffolds with the surrounding calvarial bone. The amount of new bone formed in the defects was dependent on the implantation time and on the scaffold group.

At 6 weeks, the amount of new bone in the as-fabricated scaffolds was limited to the periphery of the scaffolds and to “islands” within the pores of the scaffolds (**Fig. 2a1**). Bone regeneration was considerably greater in the defects implanted with pretreated and the BMP2-loaded scaffolds, with the new bone bridging the edges of the defect (**Fig. 2a2, 2a3**). The amount of new bone in the defects implanted with the pretreated scaffolds was not significantly different from that for the BMP2-loaded scaffolds. The as-fabricated and pretreated scaffolds contained a significantly higher amount of fibrous tissue than the BMP2-loaded scaffolds whereas the BMP2-loaded scaffolds had a significantly higher fraction of bone marrow-like tissue than the as-fabricated and pretreated scaffolds.

As the implantation time increased to 12 and 24 weeks, the stained sections (**Fig. 2b1-2c3**) consistently showed an increase in new bone in the defects implanted with the

as-fabricated and BMP2-loaded scaffolds while the amount of new bone varied over a wide range for the pretreated scaffolds. The new bone almost completely infiltrated the pores of the BMP2-loaded scaffolds within 12 weeks. The amount of marrow-like tissue observed at 6 weeks in the defects implanted with the BMP2-loaded scaffolds decreased markedly with the increase in implantation time. Higher magnification images of the stained sections at 24 weeks (**Fig. 2d1-2d3**) showed that for all three groups of scaffolds, the new bone was composed of lamellar bone, similar to host bone, and that it adhered tightly to the surface of the scaffolds.

Since all the scaffolds had the same microstructure, their capacity to regenerate bone in the defects was compared by normalizing the amount of new bone to the total pore space (area) of the scaffolds (**Fig. 3**). The amount of new bone in the as-fabricated scaffolds increased significantly from $45 \pm 11\%$ at 6 weeks to $58 \pm 6\%$ at 24 weeks. While the amount of new bone in the pretreated scaffolds at 6 weeks ($64 \pm 9\%$) was significantly higher than that in the as-fabricated scaffolds, there was little increase with longer implantation time. The amount of new bone in the pretreated scaffolds at 24 weeks ($67 \pm 9\%$) was not significantly higher than that in the as-fabricated scaffolds at the same implantation time. In comparison, the amount of new bone in the BMP2-loaded scaffolds increased significantly from $73 \pm 8\%$ at 6 weeks to $95 \pm 3\%$ at 24 weeks and was significantly greater than that in the as-fabricated scaffolds at all three implantation times. The amount of new bone in the BMP2-loaded scaffolds was also significantly greater than that in the pretreated scaffolds at 12 and 24 weeks.

3.2 Assessment of bone marrow and fibrous tissue

Previously, at 6 weeks post-implantation, it was found that for the as-fabricated and pretreated scaffolds, the pore space that was not infiltrated with new bone was filled mainly with fibrous (soft) tissue [10]. In comparison, the BMP2-loaded scaffolds contained a significantly greater amount of bone marrow-like tissue but a significantly smaller amount of fibrous tissue. Although the mechanism is not clear, marrow-rich bone is observed to be a typical outcome of BMP2-induced bone growth [13–15]. In the present study, the amount of bone marrow-like tissue in the BMP2-loaded scaffolds at 6 weeks post-implantation ($22 \pm 8\%$ of the pore space of the scaffolds) decreased significantly at 12 and 24 weeks post-implantation (**Fig. 4a**). At 12 and 24 weeks, the pore space was almost completely filled with lamellar bone (**Fig. 2c3**), indicating that the marrow-like tissue had converted to mature bone. The amount of fibrous tissue in the as-fabricated and pretreated scaffolds decreased more slowly as the implantation time increased from 6 weeks to 24 weeks (**Fig. 4b**).

3.3 Assessment of mineralized tissue and bioactive glass conversion

Transmitted light images of von Kossa stained sections of the rat calvarial defects implanted for 12 and 24 weeks with the as-fabricated, pretreated and BMP2-loaded scaffolds are shown in **Fig. 5**. Images of the defects implanted for 6 weeks with the three groups of scaffolds [10] are included for comparison. The von Kossa staining detects a combination of bone and glass converted to HA (or phosphate material). For all three groups of scaffolds, the total von Kossa-positive area increased as the implantation time increased from 6 weeks to 24 weeks. The increase was particularly noticeable for the

defects implanted with the BMP2-loaded scaffolds which showed a considerable amount of von Kossa-positive area (**Fig. 5c3**).

The total von Kossa-positive area, evaluated as a fraction of the total defect area, was $38 \pm 9\%$, $56 \pm 4\%$ and $59 \pm 5\%$, respectively for the as-fabricated, pretreated and BMP2-loaded scaffolds at 6 weeks post-implantation (**Fig. 6a**). At 24 weeks, the total von Kossa-positive area increased to $57 \pm 6\%$, $64 \pm 5\%$ and $81 \pm 4\%$, respectively, for the as-fabricated, pretreated, and BMP2-loaded scaffolds. The increase in the total von Kossa-positive area from 6 to 24 weeks was significant for each group of scaffolds but the magnitude of the increase was smaller for the pretreated scaffolds.

To evaluate how much of the von Kossa-positive area was attributed to the converted glass alone, the percent new bone determined from the H&E stained sections (as a fraction of the total defect area) was subtracted from the total von Kossa-positive area. The percent von Kossa-positive area due to the glass conversion to HA (evaluated as a fraction of the total defect area) was $17 \pm 3\%$, $24 \pm 2\%$ and $24 \pm 3\%$, respectively for the as-fabricated, pretreated and BMP2-loaded scaffolds at 6 weeks post-implantation (**Fig. 6b**). At 24 weeks, the von Kossa-positive area due to the glass conversion increased to $29 \pm 3\%$, $31 \pm 2\%$ and $34 \pm 4\%$, respectively, for the as-fabricated, pretreated and BMP2-loaded scaffolds. The increase in the von Kossa-positive area due to the glass conversion from 6 weeks to 24 weeks was significant for each group of scaffolds but at 24 weeks, there was no significant difference among the von Kossa-positive area due to the glass conversion for the three groups of scaffolds.

3.4. SEM evaluation of implants

Figure 7 shows backscattered SEM images of the rat calvarial defects implanted with the bioactive glass scaffolds at 24 weeks. Images of the defects implanted with the scaffolds at 12 weeks showed similar features and they are omitted for brevity. The cracks in the sections and the delamination of the converted glass layer from the scaffolds are presumably due to mechanical stresses resulting from grinding to attain a flat surface and capillary stresses during the preparation (drying) of the sections for SEM analysis. The contrast in the grayscale images is an indication of differences in the calcium content. The unconverted glass, the converted surface layer and the new bone, all with higher calcium content, had a light gray color. In comparison, the silica-rich layer, formed in the early stage of the glass conversion process, was dark gray. Lacunae within the bone, fibrous tissue and bone marrow-like tissue were almost black. The filaments in the scaffolds showed a considerable amount of unconverted glass even at 24 weeks post-implantation, due to the well-known slow conversion of 13-93 bioactive glass [2].

New bone appeared to bond tightly to the surface of the converted layer for all three groups of scaffolds at 24 weeks post-implantation. This was also found at 12 weeks for all three groups of scaffolds (results not included), and for the pretreated and BMP2-loaded scaffolds at 6 weeks [10]. New bone did not appear to bond to the as-fabricated scaffolds at 6 weeks. Instead, the new bone formed “islands” within the pores of the scaffolds and there were large gaps between the newly formed bone and the converted surface of the scaffold.

The average thickness of the converted layer of the three groups of scaffolds at 24 weeks post-implantation, determined from the SEM images (**Fig. 7**), was approximately

30, 20 and 20 μm , respectively, for the as-fabricated, pretreated, and BMP2-loaded scaffolds. The Ca/P atomic ratio of the converted layer, silica-rich layer and unconverted glass of the scaffolds and the Ca/P atomic ratio of the new bone in the defects at 12 weeks and 24 week post-implantation, determined using EDS analysis, are summarized in **Table I**. The Ca/P atomic ratio of the converted layer for the three groups of scaffolds did not show a significant change as the implantation time increased from 12 to 24 weeks. At 24 weeks, the Ca/P atomic ratio of the converted layer was 1.62 and 1.66, respectively, respectively, for the as-fabricated, and BMP2-loaded scaffolds which were not significantly different from the value (1.67) for a stoichiometric HA. However, the Ca/P atomic ratio for the converted layer of the pretreated scaffolds at 24 weeks (1.54) was smaller than that for stoichiometric HA.

3.5 Assessment of angiogenesis

Transmitted light images of H&E and PAS stained sections showed that blood vessels infiltrated the defects implanted with all three groups of scaffolds. Because they provided more definitive detection of the micro-vessels, the PAS stained images were used to assess the area and number of blood vessels in the defects. Blood vessels were observed in the new bone, fibrous (soft) tissue and marrow-like tissue. As described earlier, the defects implanted for 6 weeks with the as-fabricated and pretreated scaffolds were also infiltrated with a considerable amount of fibrous (soft) tissue whereas the defects implanted with the BMP2-loaded scaffolds also contained a considerable amount of marrow-like tissue. A large number of blood vessels was observed in the marrow-like tissue at 6 weeks. Because of the difference in the amount of fibrous and marrow-like tissue in the three

groups of scaffolds, the blood vessel area and the number of blood vessels were evaluated in the new bone only.

Figure 8 shows images of PAS stained sections of the defects implanted with the three groups of scaffolds at 12 weeks post-implantation. Images for implantation times of 6 weeks and 24 weeks are omitted for brevity. At 6 weeks post-implantation, sparse capillary vessels were observed within the new bone in the as-fabricated scaffolds but a larger number of capillaries were found in the pretreated scaffolds and particularly in the BMP2-loaded scaffolds. At 12 weeks, along with the increase in new bone described earlier, there was an increase in the number of capillaries in the defects implanted with the BMP2-loaded scaffolds (**Fig. 8c1**). With an increase in the implantation time to 24 weeks, the morphology and color of the bone in the scaffolds were comparable to host bone, indicating good maturity of the infiltrated bone. The number and size of the blood vessels appeared to be similar to those in the host bone.

The percent blood vessel area in the defects implanted with the three groups of scaffolds, determined as a fraction of the new bone area, is shown in **Fig. 9a** at 6, 12, and 24 weeks post-implantation. At 6 weeks, the BMP2-loaded scaffolds had the highest percentage of blood vessel area within the defect ($4.6 \pm 0.5\%$) which was significantly higher than the values for the as-fabricated scaffolds ($2.4 \pm 0.3\%$) and the pretreated scaffolds ($2.7 \pm 0.3\%$). The percent blood vessel area in the BMP2-loaded scaffolds decreased significantly to $3.1 \pm 0.5\%$ at 12 weeks but it was still significantly higher than the value for the as-fabricated scaffolds ($2.0 \pm 0.4\%$) and higher than that for the pretreated scaffolds ($2.3 \pm 0.4\%$). The blood vessel area in those two groups was comparable to the value ($\sim 2\%$) observed in scaffolds of 13-93 glass with a fibrous microstructure implanted

for 12 weeks in the same animal model [16]. The percent blood vessel area at 24 weeks was $2.0 \pm 0.2\%$, $2.0 \pm 0.3\%$ and $2.1 \pm 0.3\%$, respectively, for the as-fabricated, pretreated and BMP2-loaded scaffolds which was approximately the same as the value in host bone ($1.9 \pm 0.3\%$).

The number of blood vessels per unit area (mm^2) of the new bone in the defects implanted with the three groups of scaffolds was also determined (**Fig. 9b**). At 6 weeks, the number of blood vessels in the BMP2-loaded scaffolds (34 ± 10) was significantly higher than in the as-fabricated scaffolds (20 ± 4) and higher than in the pretreated scaffolds (29 ± 9). The blood vessel number in the BMP2-loaded scaffolds increased to 44 ± 12 at 12 weeks, whereas the vessel number in the as-fabricated scaffolds (18 ± 6) and the pretreated scaffolds (25 ± 6) were comparable to the values at 6 weeks. At 24 weeks, the blood vessel number within the new bone was 16 ± 5 , 19 ± 4 and 25 ± 7 , respectively, for the as-fabricated, pretreated and BMP2-loaded scaffolds. The differences among the groups were not significant.

4. Discussion

There is growing interest in the use of bioactive glass to heal bone defects. However, most previous *in vivo* studies have utilized bioactive glasses in the form of particles or weak porous 3D scaffolds and implantation times of 12 weeks or shorter. The significant features of the present study included the use of strong porous scaffolds that may have potential in healing large (critical size) defects in loaded or non-loaded bone and longer implantation times (12 and 24 weeks). Previously, we found that that pretreating as-fabricated 13-93 bioactive glass scaffolds of in an aqueous phosphate solution to convert a thin surface layer to HA or loading the pretreated scaffolds with BMP2 significantly

enhanced their capacity to regenerate bone at 6 weeks. A key objective of the present study was to determine whether the promising bone regeneration observed at 6 weeks continued to longer implantation periods and to understand the processes that influence the long-term healing of bone defects implanted with 13-93 glass scaffolds.

The amount of new bone in the rat calvarial defects implanted with the as-fabricated scaffolds increased with time and, at 24 weeks, the amount of new bone was significantly greater than that at 6 weeks (**Fig. 3**). In comparison, the significant enhancement in bone regeneration observed previously at 6 weeks in the defects implanted with the pretreated scaffolds appeared to be a short-term effect. There was little increase in the amount of new bone in the defects implanted with the pretreated scaffolds at 12 and 24 weeks. The significant difference between the as-fabricated and pretreated scaffolds to regenerate bone at 6 weeks was previously discussed in terms of their different surface characteristics [10]. Upon implantation, the surface of the pretreated scaffolds was composed of a high-surface-area mesoporous ACP or HA material whereas the as-fabricated scaffolds was composed of a dense silicate glass. This difference in surface characteristics could initially influence the response of cells. Subsequently, the as-fabricated scaffolds converted faster to ACP or HA when compared to the pretreated scaffolds. After the formation of the ACP or HA surface layer, presumably the faster conversion of the as-fabricated scaffolds served to improve their capacity to regenerate bone. Thus, by 24 weeks, there was no significant difference in bone regeneration between the as-fabricated and pretreated scaffolds.

The BMP2-loaded scaffolds showed the best capacity to regenerate bone. The pore space within the scaffolds was almost completely infiltrated with lamellar bone within 12 weeks. Loading the 13-93 bioactive glass scaffolds with BMP2 could provide a promising

method for enhancing their capacity to regenerate sufficient bone within a clinically relevant time. The amount of BMP2 loaded into each scaffold (1 μg per defect or 60 ng per mm^3) was well below the value (>120 ng/mm^3) required for bridging 5 mm defects using 3D poly(lactic-co-glycolic acid) scaffolds [17] and the value (250 ng/mm^3) observed to cause adverse biological effects in the same animal model [18]. In the present study, no adverse biological effects were observed in the H&E stained sections of the defects implanted with the three groups of scaffolds for the three implantation times used.

The defect size (4.6 mm) used in the present study is not a critical size defect in the rat calvarial model. However, a defect size of ~ 5 mm in this animal model has been used often to evaluate the response of biomaterials in osseous defects. The defect size in the present study was based on the diameter of a commercially available trephine drill and the use of bilateral defects (one defect in the central area of each parietal bone of the calvaria). For an unfilled defect of that size, our previous study showed that only a thin layer of new bone was formed at the defect margin at 12 weeks and most of the defect was filled with compressed fibrous connective tissue [19]. The thin layer of bone formed after 12 weeks failed to bridge the defect at after 24 weeks. Thus the healing of the defects observed in the present study can be attributed mainly to the capacity of the BMP2-loaded scaffolds to stimulate osteogenesis.

The release profile of BMP2 from the scaffolds into a medium composed of fetal bovine serum and phosphate-buffered saline, measured previously [10], showed that $\sim 10\%$ of the BMP2 loaded into the scaffolds was released over the first 3–4 days and that the release of BMP2 almost ceased thereafter. Despite this limited short-term release of BMP2 observed *in vitro*, the results of the present study showed a significant capacity of the

BMP2-loaded scaffolds to enhance bone regeneration for up to 24 weeks *in vivo*. A thin surface layer of the scaffolds was converted to a high-surface-area hydroxyapatite (30 ± 3 m²/g) that served as a substrate for the BMP2. Because of the high affinity of BMP2 for HA, its release rate from HA *in vitro* is often low. The adsorbed BMP2 is reported to be strongly immobilized on the surface of the HA by electrostatic and other interactions, such as hydrogen bonding [20]. This strong interaction makes it difficult for the BMP2 to be displaced from the HA surface by competitive adsorption from other proteins [21]. However, a greater release of BMP2 from the scaffolds can be expected *in vivo* because of a higher degradation rate of the HA surface layer due to cell-mediated degradation in addition to dissolution-mediated degradation [22, 23] and the higher solubility of proteins *in vivo*. Presumably the BMP2 release *in vivo* was above the threshold required to stimulate bone regeneration over a period that was much longer than the release time observed *in vitro*.

An attractive property of bioactive glasses is their ability to convert to HA which leads to a strong bond with bone. The rate of conversion to HA depends primarily on the bioactive glass composition, the medium (*in vitro* versus *in vivo*) and the architecture of the glass (porosity, pore size and pore interconnectivity) [16, 19, 24–27]. As the bioactive glass scaffold converts to HA, its strength decreases [9, 19]. Consequently, the application of bioactive glass scaffolds in structural or loaded bone repair depends not only on the strength of the as-fabricated scaffold but also on the relative rates of conversion (degradation in strength) and new bone infiltration (enhancement in strength). A requirement for structural bone repair is to avoid rapid degradation in the strength prior to sufficient new bone infiltration. The slow conversion rate of silicate 13-93 bioactive glass

scaffolds to HA is an advantage for the retention of strength. The amount of glass conversion at 24 weeks, determined by subtracting the percent new bone in the defects from the total von Kossa-positive area was 30–33% for the three groups which showed that the pretreatment or BMP2 loading had little long-term effect on conversion of the scaffolds in the defects. If required, more rapid conversion of the 13-93 scaffolds to HA can be achieved by reducing the diameter of the glass filaments in the grid-like architecture (Fig. 1).

Angiogenesis is essential for bone formation and growth, and it plays a critical role in bone defect repair [28]. Blood vessels provide a means for tissues to receive oxygen and various nutrients. The relationship between angiogenesis and osteogenesis is well recognized [29]. The vasculature penetrates into the bioactive glass scaffold and enables numerous cells and tissues to receive nourishment. The enhancement of angiogenesis increases bone regeneration [30]. In the present study, the area and number blood vessels in the new bone that infiltrated the BMP2-loaded scaffolds at 6 and 12 weeks were significantly greater than those for the as-fabricated or pretreated scaffolds, showing the capacity of the BMP2-loaded scaffolds to enhance angiogenesis. The blood vessel area and number showed a decreasing trend with time and became comparable to the values in host bone within 24 weeks.

Together, the results of the present study showed that loading the 13-93 bioactive glass scaffolds with a moderate amount of BMP2 (1 μg per defect) resulted in their ability to stimulate osteogenesis and angiogenesis in a rat calvarial defect model, particularly at shorter implantation times (<12 weeks). Extensive data have shown that BMPs, particularly BMP2, can initiate the complete cascade of bone formation, including the

migration of mesenchymal stem cells and their differentiation into pre-osteoblasts and then into osteoblasts [31, 32]. While several growth factors can play a role in angiogenesis, vascular endothelial growth factor (VEGF) is considered to be a key regulator of angiogenesis during bone regeneration [33]. Studies have shown that BMP-induced differentiation of pre-osteoblast-like cells can enhance the production of VEGF by the resulting osteoblasts [34, 35]. The simultaneous delivery or expression of BMP and VEGF has been shown to result in enhanced bone formation *in vivo* [36–38]. In the present study, presumably enhanced production of VEGF by the osteoblasts stimulated angiogenesis and this, coupled with the continuous release of BMP2 from the scaffolds, served to enhance new bone formation in the defects.

5. Conclusions

Bone regeneration in rat calvarial defects implanted with strong porous bioactive glass (13-93) scaffolds was studied at implantation times of 12 and 24 weeks and compared with a similar study at 6 weeks. Bone regeneration in the defects implanted with the as-fabricated scaffolds increased significantly with increase in the implantation time from 6 to 24 weeks. Pretreating the scaffolds to convert a thin surface layer to hydroxyapatite enhanced bone regeneration at 6 weeks but not at 12 or 24 weeks. Scaffolds loaded with BMP2 (1 $\mu\text{g}/\text{defect}$) significantly enhanced bone regeneration at all three implantation times. The pore space of the BMP2-loaded scaffolds was almost completely infiltrated with lamellar bone within 12 weeks. The pretreatment or BMP2 loading did not affect the amount of bioactive glass converted to hydroxyapatite at 24 weeks (~30%). While blood vessels were present in the new bone that infiltrated all three groups of scaffolds, the BMP2-loaded scaffolds had a significantly higher number of blood vessels and blood

vessel area at 6 and 12 weeks post-implantation. Strong porous bioactive glass (13-93) scaffolds loaded with clinically acceptable levels of BMP2 could provide promising implants for healing structural (loaded) bone defects within a clinically relevant time.

Acknowledgements

This work was supported by the Center for Biomedical Science and Engineering, Missouri University of Science and Technology. The authors thank Mo-Sci Corp., Rolla, MO for the bioactive glass used in this work and the Phelps County Regional Medical Center, Rolla, MO for assistance with H&E staining.

References

- [1] Gerhardt LC, Boccaccini AR. Bioactive glass and glass-ceramic scaffolds for bone tissue engineering. *Materials (Basel)*. 2010;3:3867–910.
- [2] Rahaman MN, Day DE, Bal BS, Fu Q, Jung SB, Bonewald LF, et al. Bioactive glass in tissue engineering. *Acta Biomater*. 2011;7:2355–73.
- [3] Baino F, Vitale-Brovarone C. Three-dimensional glass-derived scaffolds for bone tissue engineering: current trends and forecasts for the future. *J Biomed Mater Res A*. 2011;97:514–35.
- [4] Jones JR. Review of bioactive glass: from Hench to hybrids. *Acta Biomater*. 2013;9:4457–86.
- [5] Fu Q, Saiz E, Rahaman MN, Tomsia AP. Bioactive glass scaffolds for bone tissue engineering: state of the art and future perspectives. *Mater Sci Eng C*. 2011;31:1245–56.
- [6] Huang TS, Rahaman MN, Doiphode ND, Leu MC, Bal BS, Day DE, et al. Porous and strong bioactive glass (13–93) scaffolds fabricated by freeze extrusion technique. *Mater Sci Eng C* 2011;31:1482–9.
- [7] Deliormanlı AM, Rahaman MN. Direct-write assembly of silicate and borate bioactive glass scaffolds for bone repair. *J Euro Ceram Soc* 2012;32:3637–46.

- [8] Fu Q, Saiz E, Tomsia AP. Direct ink writing of highly porous and strong glass scaffolds for load-bearing bone defects repair and regeneration. *Acta Biomater* 2011;7:3547–54.
- [9] Liu X, Rahaman MN, Hilmas GE, Bal BS. Mechanical properties of bioactive glass scaffolds fabricated by robotic deposition for structural bone repair. *Acta Biomater* 2013;9:7025–34.
- [10] Liu X, Rahaman MN, Liu Y, Bal BS, Bonewald LF. Enhanced bone regeneration in surface-modified and BMP-loaded bioactive glass (13-93) scaffolds in a rat calvarial defect model. *Acta Biomater* 2013;9:7506–17.
- [11] Bi L, Zobell B, Liu X, Rahaman MN, Bonewald LF. Healing of critical-size segmental defects in rat femora using strong porous bioactive glass scaffolds. *Mater Sci Eng C* 2014;42:816–24.
- [12] Liu W-C, Robu IS, Patel R, Leu MC, Velez M, Chu T-M G. The effects of 3D bioactive glass scaffolds and BMP-2 on bone formation in rat femoral critical size defects and adjacent bones. *Biomed Mater* 2014;9:045013 (11pp).
- [13] Hayashi C, Hasegawa U, Saita Y, Hemmi H, Hayata T, Nakashima K, et al. Osteoblastic bone formation is induced by using nanogel-crosslinking hydrogel as novel scaffold for bone growth factor. *J Cell Physiol* 2009;220:1–7.
- [14] Hong S-J, Kim C-S, Han D-K, Cho I-H, Jung U-W, Choi S-H, et al. The effect of a fibrin-fibronectin/ β -tricalcium phosphate/recombinant human bone morphogenetic protein-2 system on bone formation in rat calvarial defects. *Biomaterials* 2006;27:3810–16.
- [15] Chung Y-I, Ahn K-M, Jeon S-H, Lee S-Y, Lee J-H, Tae G. Enhanced bone regeneration with BMP-2 loaded functional nanoparticle–hydrogel complex. *J Control Release* 2007;121:91–9.
- [16] Bi L, Jung S, Day D, Neidig K, Dusevich V, Eick D, Bonewald L. Evaluation of bone regeneration, angiogenesis, and hydroxyapatite conversion in critical-sized rat calvarial defects implanted with bioactive glass scaffolds. *J Biomed Mater Res A* 2012;100:3267–75.
- [17] Cowan CM, Aghaloo T, Chou YF, Walder B, Zhang X, Soo C, et al. MicroCT evaluation of three-dimensional mineralization in response to BMP-2 doses *in vitro* and in critical sized rat calvarial defects. *Tissue Eng* 2007;13:501-12.
- [18] Zara JN, Siu RK, Zhang X, Shen J, Ngo, Lee M, et al., High doses of bone morphogenetic protein 2 induce structurally abnormal bone and inflammation *in vivo*, *Tissue Eng A* 2011;17:1389–99.

- [19] Liu X, Rahaman MN, Fu Q. Bone regeneration, mineralization, and mechanical response of bioactive glass (13-93) scaffolds with oriented and trabecular microstructures implanted in rat calvarial defects. *Acta Biomater* 2013;9:4889–98.
- [20] Boix T, Gomez-Morales J, Torrent-Burgues J, Monfort A, Puigdomenech P, Rodriguez-Clemente R. Adsorption of recombinant human bone morphogenetic protein rhBMP-2 onto hydroxyapatite. *J Inorg Biochem* 2005;99:1043–50.
- [21] Ruhe PQ, Boerman OC, Russel FG, Mikos AG, Spauwen PH, Jansen JA. *In vivo* release of rhBMP-2 loaded porous calcium phosphate cement pretreated with albumin. *J Mater Sci Mater Med* 2006;17:919–27.
- [22] Doi Y, Iwanaga H, Shibutani T, Moriwaki Y, Iwayama Y: Osteoclastic responses to various calcium phosphates in cell cultures. *J Biomed Mater Res* 1999;47:424–33.
- [23] Leeuwenburgh S, Layrolle P, Barrère F, de Bruijn J, Schoonman J, van Blitterswijk CA, de Groot K. Osteoclastic resorption of biomimetic calcium phosphate coatings *in vitro*. *J Biomed Mater Res* 2001;56:208–15.
- [24] Yao A, Wang D, Huang H, Fu Q, Rahaman MN, Day DE. *In vitro* bioactive characteristics of borate-based glasses with controllable degradation behavior. *J Am Ceram Soc* 2007;90: 303–6.
- [25] Fu Q, Rahaman MN, Fu H, Liu X. Silicate, borosilicate, and borate bioactive glass scaffolds with controllable degradation rate for bone tissue engineering applications. I. Preparation and *in vitro* degradation. *J Biomed Mater Res A* 2010;95:164–71.
- [26] Fu Q, Rahaman MN, Fu H, Liu X. Silicate, borosilicate, and borate bioactive glass scaffolds with controllable degradation rate for bone tissue engineering applications. II. *In vitro* and *in vivo* biological evaluation. *J Biomed Mater Res A* 2010;95:172–9.
- [27] Bi L, Rahaman MN, Day DE, Brown Z, Samujh C, Liu X, Mohammadkhah A, Dusevich V, Eick JD, Bonewald LF. Effect of borate bioactive glass microstructure on bone regeneration, angiogenesis and hydroxyapatite conversion in a rat calvarial defect model. *Acta Biomater* 2013; 9:8015–26.
- [28] Fang TD, Salim A, Xia W, Nacamuli RP, Guccione S, Song HM et al. Angiogenesis is required for successful bone induction during distraction osteogenesis. *J Bone Miner Res* 2005;20:1114–24.
- [29] Kanczler JM, Oreffo ROC. Osteogenesis and angiogenesis: The potential for engineering bone. *Eur Cells Mater* 2008;15:100–14.
- [30] Kaigler JM, Wang D, Horger K, Mooney DJ, Kresbach PH. VEGF scaffolds enhance angiogenesis and bone regeneration in irradiated osseous defects. *J Bone Miner Res* 2006;21:735–44.

- [31] Wozney JM. Overview of bone morphogenetic proteins. *Spine* 2002;27:S2–8.
- [32] Devescovi V, Leonardi E, Ciapetti G, Cenni E. Growth factors in bone repair. *Chir Organi Mov* 2008;92:161–8.
- [33] Gerstenfeld LC, Cullinane DM, Barnes GL, Graves DT, Einhorn TA. Fracture healing as a post-natal developmental process: molecular, spatial, and temporal aspects of its regulation. *J Cell Biochem* 2003;88:873–84.
- [34] Deckers MM, van Bezooijen RL, van der Horst G, Hoogendam J, van Der Bent C, Papapoulos SE, et al. Bone morphogenetic proteins stimulate angiogenesis through osteoblast-derived vascular endothelial growth factor A. *Endocrinology* 2002;143:1545–53.
- [35] Kozawa O, Matsuno H, Uematsu T. Involvement of p70 S6 kinase in bone morphogenetic protein signaling: vascular endothelial growth factor synthesis by bone morphogenetic protein-4 in osteoblasts. *J Cell Biochem* 2001;81:430–6.
- [36] Huang YC, Kaigler D, Rice KG, Krebsbach PH, Mooney DJ. Combined angiogenic and osteogenic factor delivery enhances bone marrow stromal cell-driven bone regeneration. *J Bone Miner Res* 2005;20:848–57.
- [37] Peng H, Usas A, Olshanski A, Ho AM, Gearhart B, Cooper GM, et al. VEGF improves, whereas sFlt1 inhibits, BMP2-induced bone formation and bone healing through modulation of angiogenesis. *J Bone Miner Res* 2005;20:2017–27.
- [38] Patel ZS, Young S, Tabata Y, Jansen JA, Wong ME, Mikos AG. Dual delivery of an angiogenic and an osteogenic growth factor for bone regeneration in a critical size defect model. *Bone* 2008;43:931–40.

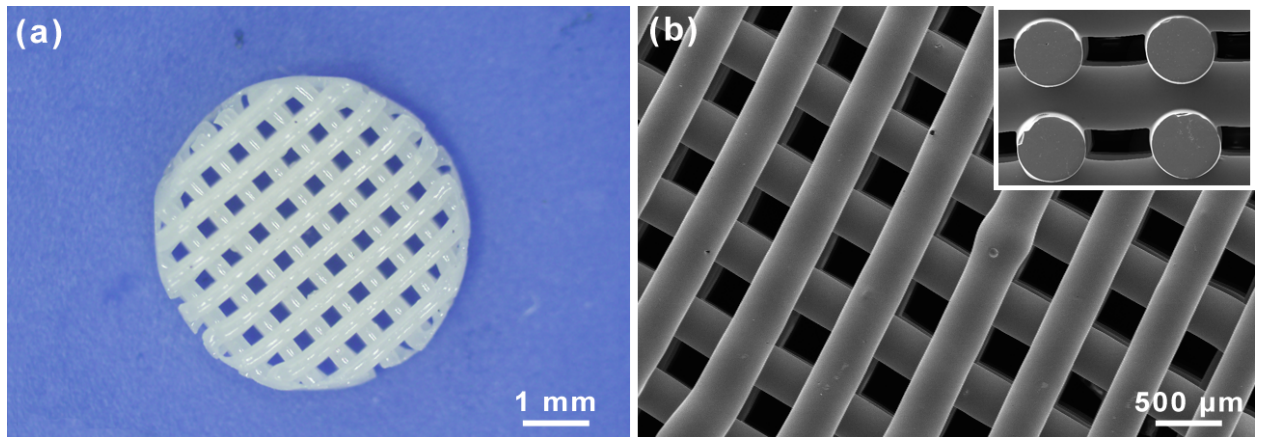


Fig. 1. (a) Optical image of 13-93 bioactive glass scaffold prepared by robocasting for implantation in rat calvarial defects [10]. (b) Higher-magnification SEM image of the scaffold showing dense glass filaments and porous grid-like architecture in the plane of deposition (xy plane). Inset: SEM image in z direction. The scaffolds had a porosity of $47 \pm 1\%$, a pore width of $300 \pm 10 \mu\text{m}$ in the xy plane and $150 \pm 10 \mu\text{m}$ in z direction.

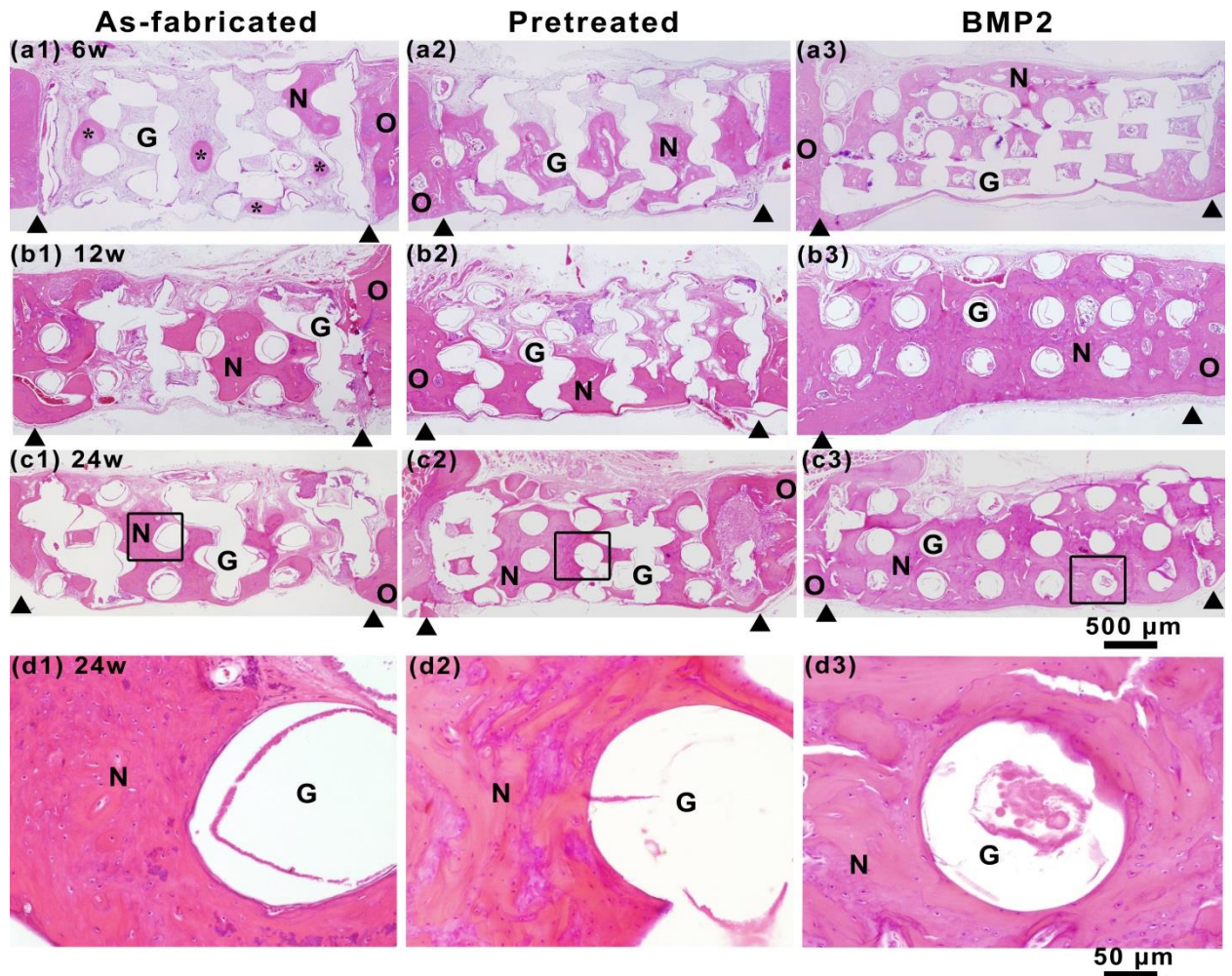


Fig. 2. Transmitted light images of H&E-stained sections of rat calvarial defects implanted for 6 weeks (a1–a3), 12 weeks (b1–b3) and 24 weeks (c1–c3) with the three groups of bioactive glass scaffolds: as-fabricated (a1–c1), pretreated (a2–c2) and BMP2-loaded (a3–c3). Higher magnification images of the boxed areas in (c1–c3) are shown in (d1–d3). N = new bone; O = host bone; * = bony island; G = bioactive glass; arrowheads indicate the edges of host bone.

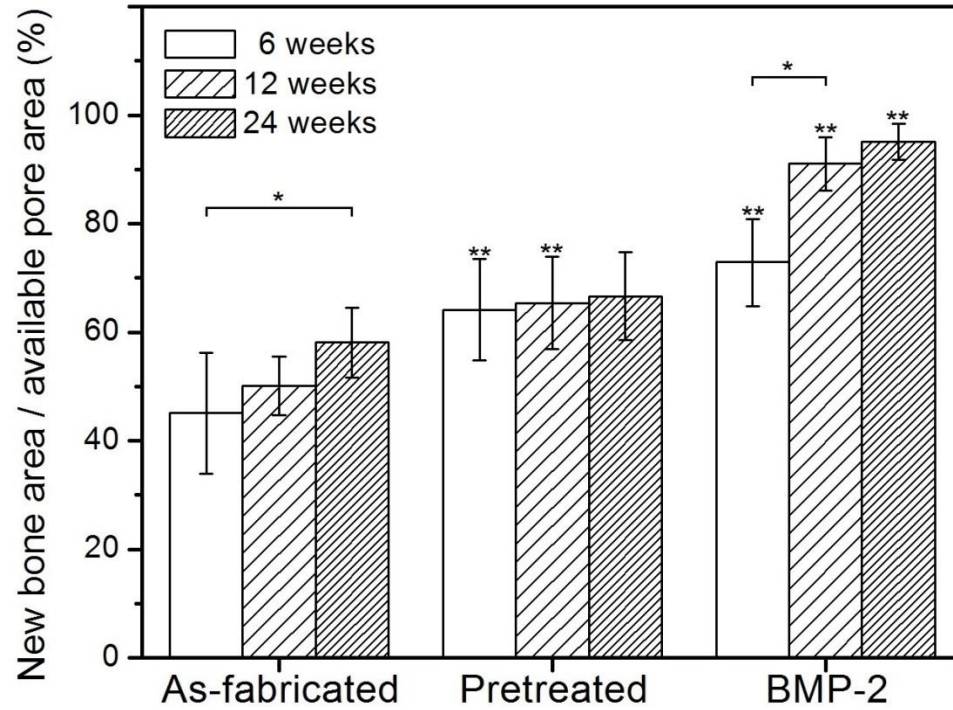


Fig. 3. Percent new bone in rat calvarial defects implanted with the three groups of scaffolds for 6, 12 and 24 weeks. The amount of new bone is shown as a percent of the available pore space (area) of the scaffolds. (*significant difference within each group; **significant difference when compared to as-fabricated scaffold at the same implantation time; $p < 0.05$)

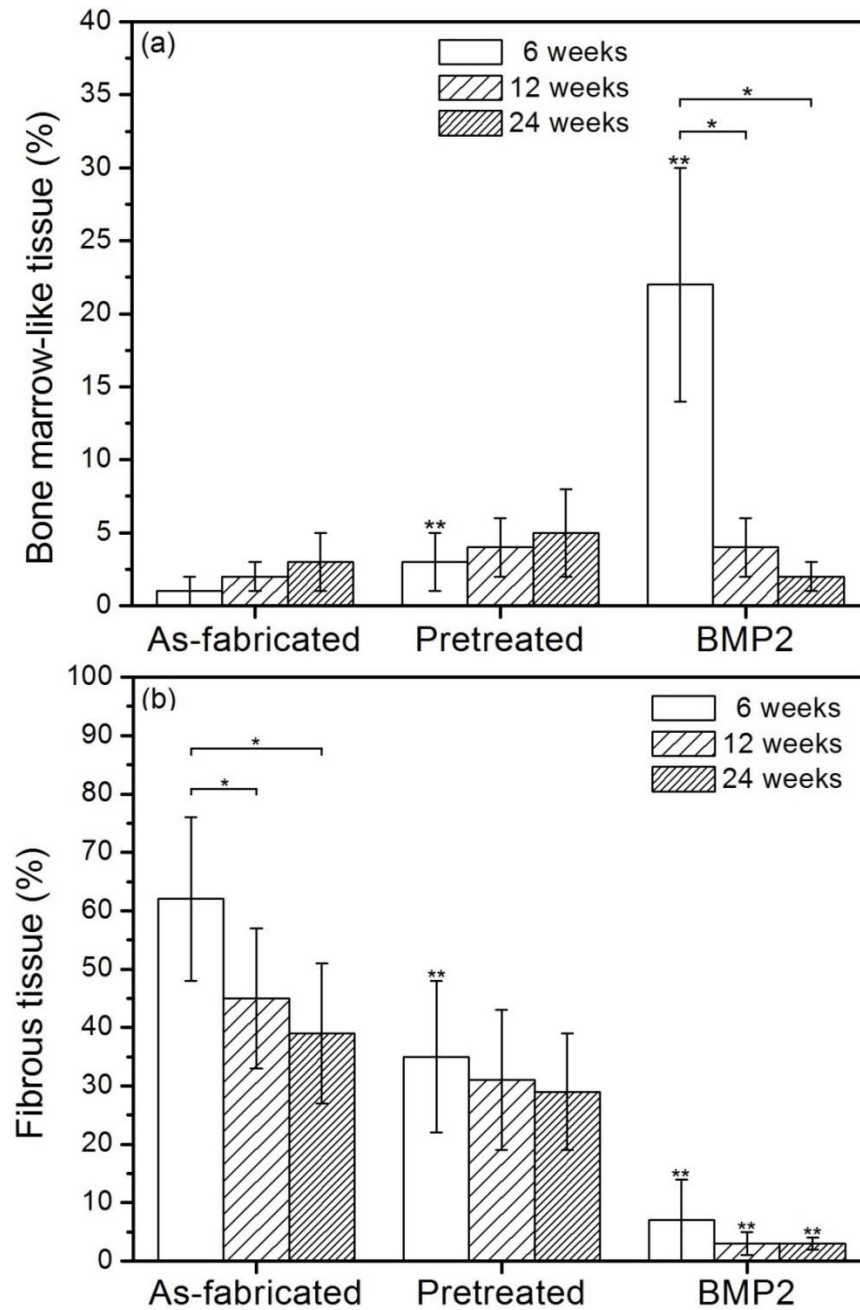


Fig. 4. Percent bone marrow-like tissue (a) and fibrous tissue (b) in rat calvarial defects implanted with the three groups of scaffolds for 6, 12 and 24 weeks. (*significant difference within each group; **significant difference when compared to as-fabricated scaffold at the same implantation time; $p < 0.05$)

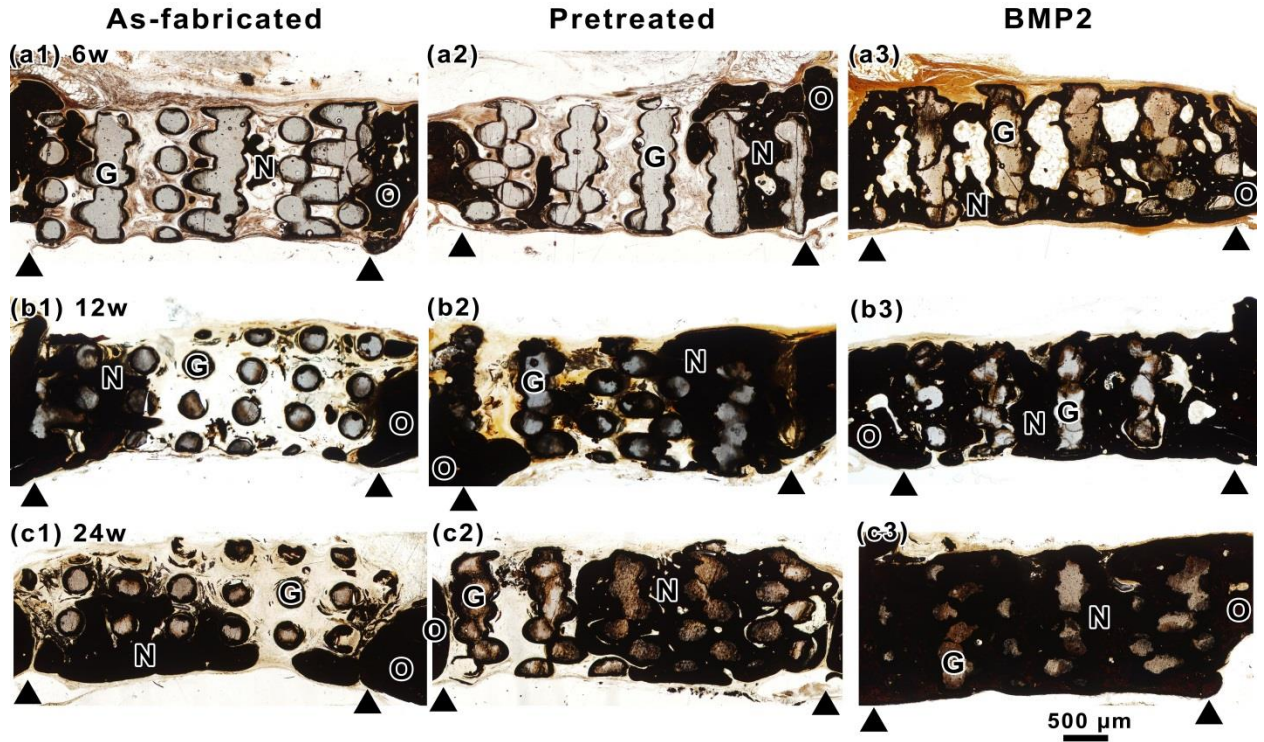


Fig. 5. Transmitted light images of von Kossa stained sections of rat calvarial defects implanted for 6 weeks (a1–a3), 12 weeks (b1–b3) and 24 weeks (c1–c3) with the three groups of bioactive glass scaffolds: as-fabricated (a1–c1), pretreated (a2–c2) and BMP2-loaded (a3–c3). N = new bone; O = host bone; G = bioactive glass; arrowheads indicate the edges of host bone.

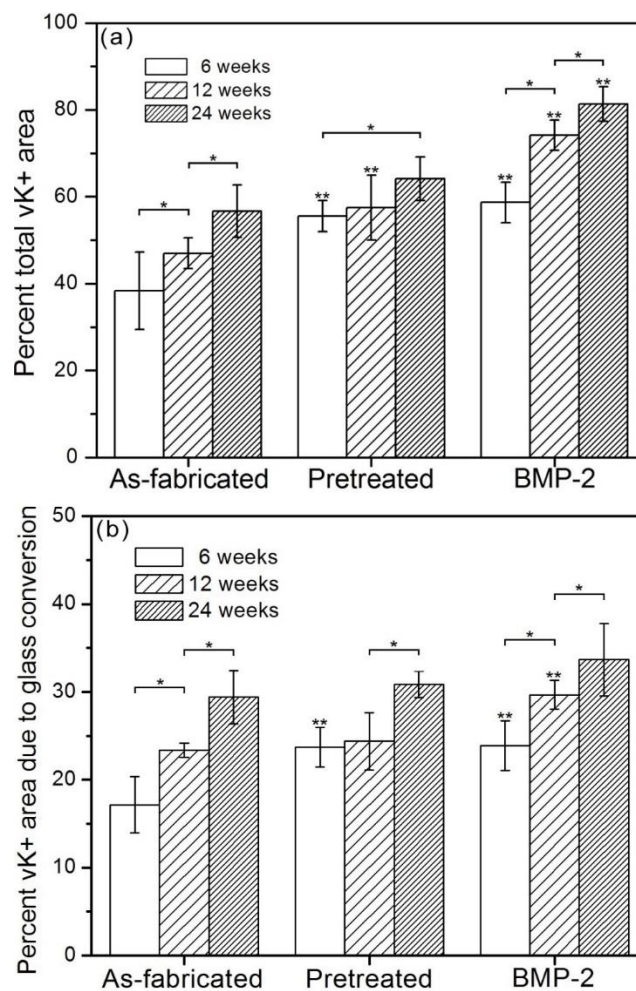


Fig. 6. Percent total von Kossa positive (vK+) area (a) and vK+ area due to the bioactive glass conversion (b), determined as a fraction of the total defect area, for rat calvarial defects implanted with the three groups of scaffolds at 6, 12 and 24 weeks post-implantation. (*significant difference within each group; **significant difference when compared to as-fabricated scaffold at the same implantation time; $p < 0.05$)

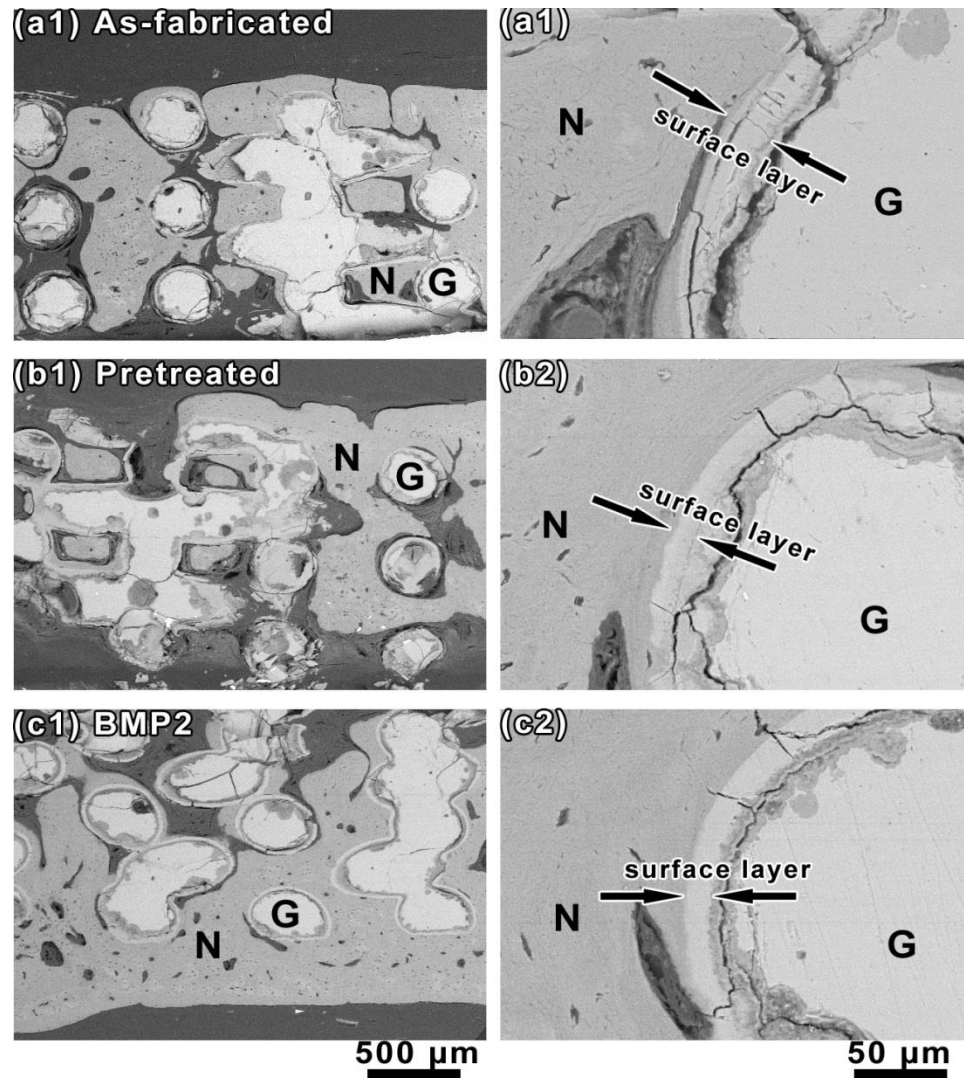


Fig. 7. Backscattered SEM images of rat calvarial defects implanted with bioactive glass scaffolds at 24 weeks post-implantation: (a1, a2) as-fabricated scaffolds; (b1, b2) pretreated scaffolds; (c1, c2) BMP2-loaded. N = new bone; G = bioactive glass. The approximate thickness of the converted surface layer on the glass filaments are shown in (a2) – (c2).

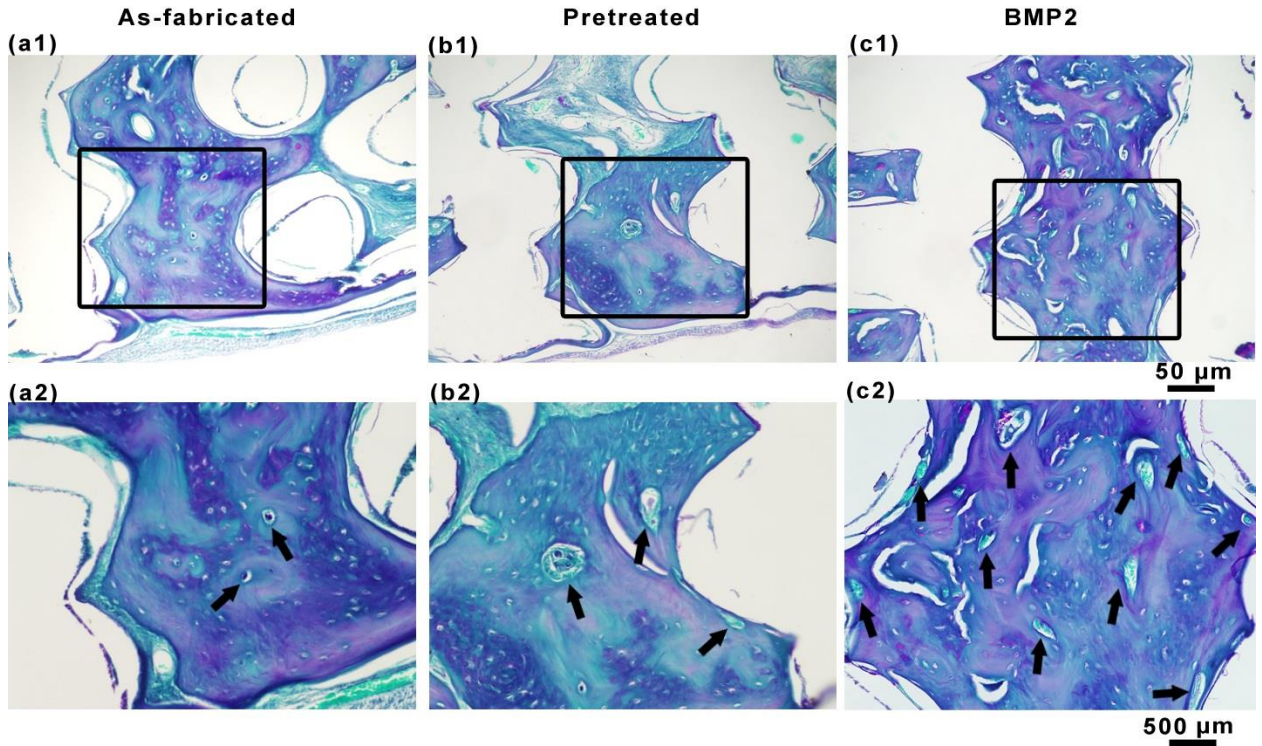


Fig. 8. Transmitted light images of PAS stained sections of rat calvarial defects implanted with the three groups of bioactive glass scaffolds at 12 weeks post-implantation: (a1, a2) as-fabricated scaffolds; (b1, b2) pretreated scaffolds; (c1, c2) BMP2-loaded scaffolds. (arrows indicate blood vessels)

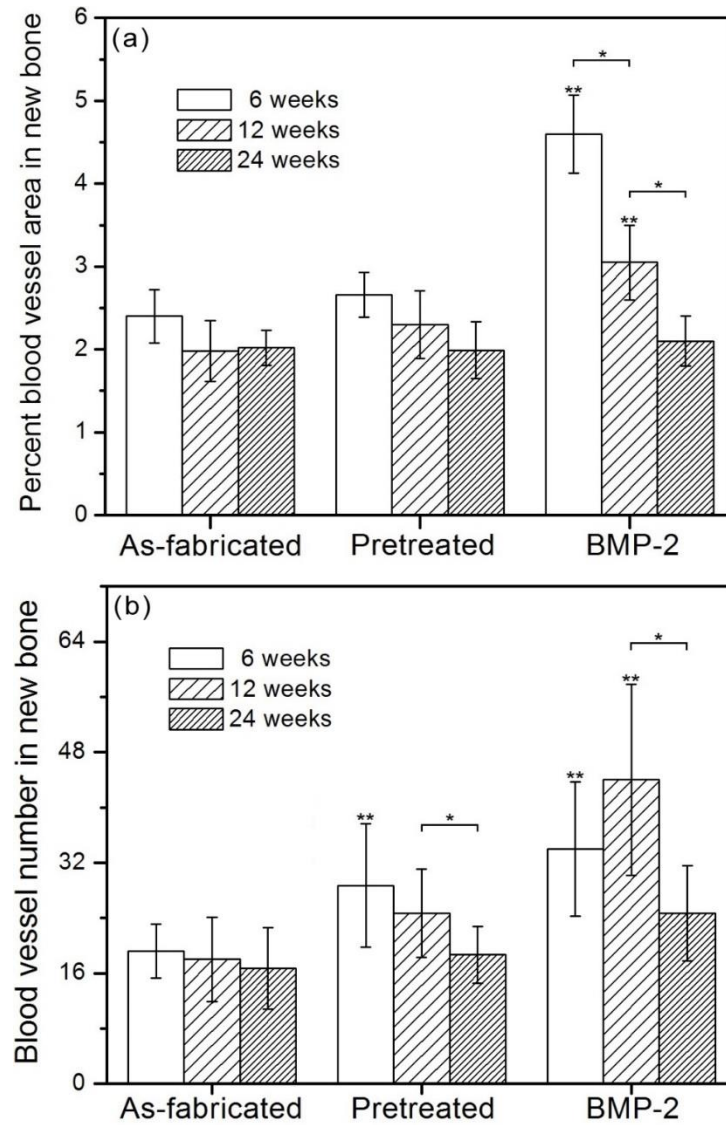


Fig. 9. (a) Percent blood vessel area and (b) number of blood vessels per unit area (mm^2) of new bone in rat calvarial defects implanted with the three groups of scaffolds at 6, 12 and 24 weeks post-implantation. (*significant difference within each group; **significant difference when compared to as-fabricated scaffold at the same implantation time; $p < 0.05$)

Table I. Calcium to phosphorus (Ca/P) atomic ratio for new bone, converted glass layer, silica-rich layer and unconverted glass in rat calvarial defects implanted with as-fabricated, pretreated and BMP2-loaded scaffolds at 12 and 24 weeks post-implantation.

Scaffold groups	Duration times (weeks)	Ca/P atomic ratio			
		New bone	Converted glass layer	Silica-rich layer	Unconverted glass
As-fabricated	12	1.72 ± 0.06	1.59 ± 0.04	2.6 ± 0.2	5.8 ± 0.3
	24	1.68 ± 0.08	1.62 ± 0.06	2.3 ± 0.1	5.4 ± 0.3
Pretreated	12	1.73 ± 0.06	1.50 ± 0.05	2.3 ± 0.2	5.6 ± 0.4
	24	1.70 ± 0.05	1.54 ± 0.07	2.2 ± 0.3	5.6 ± 0.2
BMP2-loaded	12	1.71 ± 0.06	1.61 ± 0.05	2.5 ± 0.3	5.8 ± 0.3
	24	1.69 ± 0.04	1.66 ± 0.07	2.2 ± 0.2	5.5 ± 0.4

II. Response of osteoblastic MC3T3-E1 cells and osseous defects to strong porous scaffolds of silicate 13-93 bioactive glass doped with copper

Yinan Lin¹, B. Sonny Bal², Mohamed N. Rahaman^{1,*}

¹ Department of Materials Science and Engineering, Missouri University of Science and Technology, Rolla, Missouri 65409

² Department of Orthopaedic Surgery, University of Missouri, Columbia, Missouri 65212

ABSTRACT

Copper ions are known to stimulate angiogenesis, a process that is essential for tissue regeneration, but high Cu ion concentration is toxic to cells and tissues. In the present study, porous scaffolds of silicate 13-93 bioactive glass doped with varying concentrations of Cu (0–2.0 wt. % CuO) were created by robotic deposition and their effect on the response of mouse preosteoblastic MC3T3-E1 cells *in vitro* and bone regeneration and angiogenesis in rat calvarial defects *in vivo* was investigated. When immersed in simulated body fluid (SBF) *in vitro*, the Cu-doped scaffolds released Cu ions into the medium in a dose-dependent manner and converted partially to hydroxyapatite. The number and alkaline phosphatase activity of MC3T3-E1 cells cultured on the scaffolds were not affected by CuO concentrations of 0.4 and 0.8 wt. % in the glass but they were significantly reduced by 2.0 wt. % CuO. Bone infiltration of the 13-93 scaffolds implanted for 6 weeks in rat calvarial defects (46 ± 8 % of the total pore area or volume) was not significantly affected by 0.4 or 0.8 wt. % CuO in the glass. In comparison, bone formation (0.8 ± 0.7 %) was significantly inhibited while fibrous (soft) tissue was significantly enhanced in the scaffolds doped with 2.0 wt. % CuO. The area of new blood vessels in the fibrous tissue that infiltrated the scaffolds increased with CuO content of the glass and was significantly higher for the scaffolds doped with 2.0 wt. % CuO. Loading the scaffolds with bone

morphogenetic protein-2 (BMP2) (1 $\mu\text{g}/\text{defect}$) significantly enhanced bone infiltration and reduced fibrous tissue in the scaffolds. Collectively, these results indicate that doping 13-93 bioactive glass scaffolds with up to 0.8 wt. % CuO had no significant benefit on MC3T3-E1 cell proliferation *in vitro* and bone regeneration *in vivo* whereas a CuO dopant concentration of 2.0 wt. % was toxic to cells and detrimental to bone regeneration.

1. Introduction

There is a clinical need for synthetic bioactive implants that can reliably repair large (critical size) bone defects, particularly segmental defects in load-bearing bones. Whereas contained bone defects are repairable with commercially-available, osteoconductive and osteoinductive filler materials [1, 2], the repair of large defects in structural bone is a challenging clinical problem. The available treatments such as bone allografts, autografts and porous metals are limited by costs, availability, durability, infection risk, donor site morbidity, and uncertain healing.

Ideally, synthetic implants for bone regeneration should have a combination of desirable properties [3]. They should be biocompatible, osteoconductive and osteoinductive, and they should have a porous three-dimensional (3D) architecture with interconnected porosity for tissue ingrowth and formation of capillaries [4]. Synthetic implants should also be bioactive and they should degrade or resorb at a controllable rate, comparable to the rate of bone regeneration. While the target mechanical properties are not well established, an often-used guideline is that the mechanical properties of the scaffold should match those of the host bone. Synthetic biomaterials for bone repair should also have the ability to be formed into anatomically relevant shapes by commercial methods and to be sterilized according to international standards for clinical use.

Synthetic biomaterials generally lack the osteoinductivity and osteogenicity of autogenous bone grafts, functioning mainly as osteoconductive implants. Consequently, the performance of synthetic biomaterials *in vivo* is inferior to that of autogeneous bone grafts (the gold standard for bone repair). The use of synthetic biomaterials by themselves commonly fails to produce clinically significant bone formation in a clinically relevant time [5, 6]. In practice, the addition of osteogenic growth factors to synthetic biomaterials is often needed to achieve reliable reconstruction of bone [7, 8]. Bone morphogenetic proteins (BMPs) such as BMP2, delivered typically by osteoconductive biomaterials, can induce robust bone formation and they have been used successfully in bone repair [7–9]. However, BMPs are commonly effective only when used in supra-physiological doses and this has resulted in heightened concerns about adverse biological effects *in vivo* [10, 11].

Angiogenesis is essential for bone formation and growth and plays a critical role in bone defect repair [12]. The relationship between angiogenesis and osteogenesis has been well established [13]. The vasculature transports oxygen, nutrients, soluble factors and numerous cell types to all tissues in the body. The enhancement of angiogenesis should increase osteogenesis [14]. While a variety of approaches have been developed to enhance angiogenesis by synthetic implants, a commonly-used approach is the incorporation of angiogenic factors such as vascular endothelial growth factor (VEGF), basic fibroblast growth factor (bFGF) and platelet-derived growth factor [15, 16]. However, the use of growth factors typically suffers from disadvantages such as high cost, potential adverse biological effects *in vivo* when used in supra-physiological doses and loss of bioactivity [10, 11, 17, 18].

Inorganic angiogenic factors such as Cu^{2+} ions are of interest because of their low cost, high stability and potentially better clinical safety when compared to growth factors [19–21]. Copper ions have been reported to enhance angiogenesis by stabilizing the expression of hypoxia-inducible factor (HIF-1 α), thus mimicking hypoxia, which plays a critical role in the recruitment and differentiation of cells and in blood vessel formation [19, 20]. The release of Cu^{2+} ions has been shown to stimulate the expression of proangiogenic factors such as VEGF and transforming growth factor- β (TGF- β) in wounds created in diabetic mice [22, 23]. Subcutaneous implantation of Cu-containing borate bioactive glass microfibers in rats significantly enhanced the growth of capillaries and small blood vessels when compared to silicate 45S5 bioactive glass microfibers and sham implant controls [24]. The ionic dissolution product of Cu-doped borate bioactive glass microfibers has been shown to stimulate the expression of angiogenic genes of fibroblasts *in vitro* and angiogenesis in full thickness skin wounds in rodents *in vivo* [25]. Scaffolds of a Cu-doped borosilicate bioactive glass have been shown to enhance blood vessel formation and bone regeneration in rat calvarial defects *in vivo* [26].

The attractive properties of bioactive glasses as a scaffold material for bone repair have been well described and reviewed in the literature [27, 28]. Bioactive glasses can be doped with inorganic ions such as Cu, Zn, Sr and Fe that have been reported to stimulate angiogenesis and/or osteogenesis. As the glass degrades, those ions are released at a therapeutically appropriate concentration. As described above, the release of Cu and other ions from borate and borosilicate bioactive glasses has been reported to enhance angiogenesis in soft tissue repair and both angiogenesis and osteogenesis in rat calvarial defects *in vivo*. However, borate-based bioactive glasses are not currently approved by the

US Food and Drug Administration for *in vivo* use in humans and some borate-based glasses may degrade too rapidly for applications in structural bone repair. While silicate bioactive glasses such as 45S5 and 13-93 have been used in bone repair applications for several years [28], the effects of Cu doping on their ability to stimulate angiogenesis and osteogenesis has received little attention.

The objective of the present study was to create porous scaffolds of silicate 13-93 glass doped with varying concentrations of Cu (0–2.0 wt. % CuO) and evaluate the ability of the Cu dopant to stimulate the proliferation and function of pre-osteoblastic MC3T3-E1 cells *in vitro* and bone regeneration and angiogenesis in osseous defects *in vivo*. The effect of the Cu doping on bone regeneration and angiogenesis was compared with an alternative approach based on loading the scaffolds with BMP2.

2. Materials and methods

2.1 Preparation of scaffolds

Scaffolds of the parent 13-93 glass (composition 53SiO₂, 6Na₂O, 12K₂O, 5MgO, 20CaO, 4P₂O₅; wt. %) and the 13-93 glass doped with 0.4, 0.8 and 2.0 wt. % CuO were created with a grid-like microstructure using a robotic deposition (robocasting) method described in detail elsewhere [29]. Briefly, each glass was prepared by melting the requisite amount of chemicals (Cu(NO₃)₂·2¹/₂H₂O, SiO₂, Na₂O, CaO, MgO, K₂O, P₂O₅) for 30 min in a platinum crucible at 1350 °C and quenching the molten glass between cold stainless steel plates. The crushed glass was grounded in a hardened steel container (8500 Shatterbox[®], Spex SamplePrep LLC., Metuchen, NJ) to give particles of size <50 μm. Then the particles were milled for 2 h in an attrition mill (Union Process, Inc., Akron, OH) using water as the liquid medium and ZrO₂ grinding media (3 mm in diameter) to give particles

of size $1.0 \pm 0.5 \mu\text{m}$, as measured by a laser diffraction particle size analyzer (Model LS, Beckman Coulter Inc., CA). The glass was mixed with a 20 wt. % Pluronic-127 binder solution to form a paste (40 vol. % glass particles) and extruded using a robocasting machine (RoboCAD 4.1; 3-D Inks, Stillwater, OK). After drying at room temperature, the scaffolds were heated in O_2 at a rate of $0.5 \text{ }^\circ\text{C}/\text{min}$ to burn out the processing additives, and sintered for 1 h at $700 \text{ }^\circ\text{C}$ (heating rate = $5 \text{ }^\circ\text{C}/\text{min}$) to densify the glass filaments. The as-fabricated scaffolds were sectioned and grounded to form thin discs (4.6 mm in diameter \times 1.5 mm), washed twice with deionized water and twice with anhydrous ethanol, dried in air and sterilized by heating for 12 h at $250 \text{ }^\circ\text{C}$.

Thirty-two as-fabricated scaffolds were loaded with BMP2 at a concentration of 1 μg per scaffold prior to implantation *in vivo* using a method described previously [30]. Briefly, the scaffolds were reacted for 3 days in an aqueous phosphate solution (0.25 M K_2HPO_4 solution) at $60 \text{ }^\circ\text{C}$ and a starting pH of 12.0 to convert a thin surface layer ($\sim 5 \mu\text{m}$) of the glass to HA (or amorphous calcium phosphate, ACP). The mass of the glass scaffolds to the volume of the K_2HPO_4 solution was kept constant at 1 g per 200 ml and the solution was stirred gently each day. The reacted scaffolds were removed from the solution, washed twice with deionized water, and twice with anhydrous ethanol to displace residual water from the scaffolds. Then the scaffolds were dried for at least 24 h at room temperature and stored in desiccator.

In the BMP2 loading process, a solution of BMP2 (Shenandoah Biotechnology Inc., PA) in citric acid was prepared by dissolving 10 μg of BMP2 in 100 μl sterile citric acid (pH = 3.0). Then 10 μl of the BMP2 solution was pipetted on to each scaffold (4.6 mm in diameter \times 1.5 mm). The amount of BMP2 loaded into the scaffolds was equivalent to 1

μg per bone defect (or per scaffold) in the animal model. The BMP2 solution was totally incorporated in the converted surface layer of the scaffolds and there was no visible evidence for any of the solution flowing out of the scaffolds. After loading with BMP2, the scaffolds were kept for ~ 24 h in a refrigerator at $4\text{ }^{\circ}\text{C}$ to dry them prior to implantation.

2.2 Degradation and conversion of scaffolds in simulated body fluid (SBF) in vitro

The degradation of the bioactive glass scaffolds (4.6 mm in diameter \times 1.5 mm) and their conversion to HA were studied as a function of immersion time in SBF [31] with a starting pH of 7.4. The concentration of Cu ions released from the scaffolds into the SBF during the degradation and conversion process was determined using inductively-coupled plasma optical emission spectrometry (ICP-OES). The weight loss of the scaffolds was measured as a function of time and used as a measure of the conversion of the glass to HA while the pH of the medium was measured using a pH meter, as described previously [32, 33]. A ratio of 1 g of scaffold to 100 ml of SBF was used in all of the conversion experiments. The weight loss and pH measurements at each time point were measured in triplicate and the data were expressed as a mean \pm standard deviation (SD). The formation of HA on the surface of the scaffolds was characterized using scanning electron microscopy, SEM (S-4700; Hitachi, Tokyo, Japan) and Raman spectroscopy (Horiba-Jobin Yvon, Inc., Edison, NJ). The samples were coated with Au/Pd and examined in the SEM at an accelerating voltage of 15 kV and a working distance of 12 mm. The Raman spectra of the samples were compared with a standard hydroxyapatite.

2.3 Cell culture

This *in vitro* study was performed to evaluate the effect of the Cu ions released from the scaffolds on the ability of the scaffolds to support the growth and differentiation of an established osteogenic cell line. The established MC3T3-E1 line of mouse pre-osteoblastic cells was obtained from ATCC (CRL-2593) and cultured in minimum essential medium (alpha modification; α -MEM) supplemented with 10% fetal bovine serum plus 5 $\mu\text{g ml}^{-1}$ gentamicin. This cell line has been used extensively in previous *in vitro* investigations to test the response of biomaterials to cells. Prior to cell seeding, the sterilized scaffolds were subjected to a 1 h preconditioning soak in normal medium. The conditioned scaffolds were blotted dry, rinsed twice with phosphate-buffered saline (PBS), placed on a 6 cm diameter Teflon disk, and seeded with 5×10^4 MC3T3-E1 cells suspended in 35 μl of complete medium, as in our previous studies using this cell line and bioactive glass scaffolds [34]. Following a 4 h incubation to permit cell attachment, the scaffolds with attached cells were transferred to a 24-well untreated plate with 2 ml of complete medium per well. The control group consisted of the same number of cells seeded in wells containing 2 ml of complete medium. All cell cultures were maintained at 37 °C in a humidified atmosphere of 5% CO₂, with the media changed every 2 days.

2.3.1 Cell morphology

SEM (Hitachi S-4700) was used to examine the morphology of cells adhered to the scaffolds. At culture intervals of 2, 7 and 14 days, the glass scaffolds with attached cells were removed, washed twice with warm PBS and soaked overnight in 2.5% glutaraldehyde in PBS. The fixed samples were washed 3 times with PBS, post-fixed with 1% osmium

tetroxide in PBS for 1 h, washed 3 times with PBS, dehydrated with a graded ethanol series and soaked for 10 min in hexamethyldisilazane (HMDS). Then the samples were dried in air to allow the liquid to fully evaporate, sputter-coated with Au/Pd and examined in the SEM at an accelerating voltage of 15 kV and a working distance of 12 mm.

2.3.2 Cell viability and proliferation

The proliferation of MC3T3-E1 cells on the scaffolds was assessed using a cell viability assay (Cell Counting Kit-8 (CCK-8), Dojindo Molecular Technologies, Inc., Japan). Briefly, MC3T3-E1 cells were cultured on the scaffolds ($n = 3$) using the procedure described above at an initial density of 5×10^3 cells per scaffold (as recommended in the CCK-8 assay protocol) for 2, 4, 7 and 14 days. An unseeded scaffold was used as a control. Subsequently, 360 μ l of serum-free α -MEM and 40 μ l of CCK-8 solution were added to each well at each time point and the system was incubated for 3 h at 37 °C in a humidified 5% CO₂ atmosphere. The formazan solution in the wells was extracted by pipetting gently several times and aliquots (100 μ l) from each well were transferred to a fresh 96-well plate. The absorbance of the colored formazan solution in the samples was measured using a microplate reader (FLUOstar Omega; BMG Labtech, Offenburg, Germany) at 450 nm. The results were expressed as the optical density of the aliquots minus the absorbance of the blank wells.

The effect of Cu ions released from the glass scaffolds on the viability of the MC3T3-E1 cells was evaluated using a live cell/dead cell assay. After culturing for 2, 7, 14 and 21 days using the procedure described above, the scaffolds were rinsed with warm PBS and incubated for an additional 30 min in 10 ml sterile tissue culture-grade Dulbecco's

PBS (DPBS) containing 2 μM calcein AM and 4 μM ethidium homodimer-1 (EthD-1; Life Technologies, Grand Island, NY). Images were collected under an epifluorescent microscope fitted with appropriate exciter and emitter filters to detect live (green fluorescent) and dead (red fluorescent) cells.

2.3.3 Alkaline phosphatase (ALP) activity

After culturing for 3, 7 and 14 days, the grid-like scaffolds with attached cells were removed, rinsed twice with PBS, subjected to three freeze/thaw cycles at $-80\text{ }^{\circ}\text{C}/37\text{ }^{\circ}\text{C}$, lysed in 500 μl of 0.5% Triton X-100 in PBS, and homogenized by sonication for 30 s on ice. The lysed cell suspension was spun at 3000 rpm for 10 min in a refrigerated microcentrifuge to sediment particulate debris. The ALP activity was assayed using a colorimetric p-NPP method. The absorbance was measured on a microplate reader (FLUOstar Omega; BMG Labtech, Offenburg, Germany) at 405 nm after 30 min incubation at $37\text{ }^{\circ}\text{C}$. ALP specific activity levels were quantified with a standard curve and normalized to the amount of total cellular dsDNA from the same sample. The dsDNA content was determined using a Pico Green assay (Molecular Probes). A 50 μl volume of working reagent was added to the 50 μl cell lysate of the sample and the sample was read at 485/528 nm (excitation/emission) on a fluorescence spectrophotometer (FLUOstar Omega, BMG Labtech, Offenburg, Germany). The amount of dsDNA was calculated by comparing the standard curves of the known dsDNA sample according to the protocol supplied by the manufacturer.

2.4. Evaluation of scaffolds in rat calvarial defects in vivo

All animal experimental procedures were approved by the Animal Care and Use Committee, Missouri University of Science and Technology, in compliance with the NIH Guide for Care and Use of Laboratory Animals (1985). Eight groups of scaffolds, composed of the parent 13-93 glass and the 13-93 glass doped with 0.4, 0.8 and 2.0 wt. % CuO without BMP2 plus these four groups of scaffolds loaded with BMP2 (1 μg per scaffold or defect), were implanted in bilateral defects in rat calvaria for 6 weeks. This animal model was used because it is a standard assay for evaluating the response of biomaterials in osseous defects. Eight scaffolds from each group were implanted randomly in the defects but scaffolds with and without BMP2 were not mixed in the same animal. The sample size (number of replicates per group, $n = 8$) was based on the results of a previous study for 13-93 glass scaffolds implanted for the same time in the same animal model [30] and a power analysis.

2.4.1 Animals and surgical procedure

Thirty-two male Sprague Dawley rats (3 months old; weight = 350–400 g, Harlan Laboratories Inc., USA) were maintained in the animal facility for 2 weeks to become acclimated to diet, water and housing. The rats were anesthetized with a combination of ketamine (72 mg/kg) and xylazine (6 mg/kg) and maintained under anesthesia with ether gas in oxygen. The surgical site was shaved, scrubbed with iodine and draped. Using sterile instruments and aseptic technique, a cranial skin incision was sharply made in an anterior to posterior direction along the midline. The subcutaneous tissue, musculature and periosteum were dissected and reflected to expose the calvarium. Bilateral full-thickness

defects 4.6 mm in diameter were created in the central area of each parietal bone using a saline-cooled trephine drill. The dura mater was not disturbed. The sites were constantly irrigated with sterile PBS to prevent overheating of the bone margins and to remove the bone debris. After the bilateral defect was implanted with the scaffold, the periosteum and skin were repositioned and closed using wound clips. The animals were given a dose of ketoprofen (3 mg/kg) intramuscularly and ~200 µl penicillin subcutaneously post-surgery, and monitored daily for the condition of the surgical wound, food intake, activity and clinical signs of infection. After 6 weeks, the animals were sacrificed by CO₂ inhalation, and the calvarial defect sites with surrounding bone and soft tissue were harvested for subsequent evaluation.

2.4.2 Histologic processing

The calvarial samples, including the surgical sites with surrounding bone and tissue, were fixed in 10% buffered formaldehyde for 3 days, then transferred into 70% ethanol and cut in half. Half of each sample was for paraffin embedding and the other half for methyl methacrylate embedding. The samples for paraffin embedding were de-siliconized by immersion for 2 h in 10% hydrofluoric acid, decalcified in 14% ethylenediaminetetraacetic acid (EDTA) for 4 weeks, dehydrated in a series of graded ethanol and embedded in paraffin using routine histological techniques. Then the specimens were sectioned to 5 µm using a microtome and stained with hematoxylin and eosin (H&E) and periodic acid-Schiff (PAS) staining technique. The un-decalcified samples were dehydrated in ethanol and embedded in PMMA. Sections were affixed to acrylic slides, ground down to 40 µm using a surface grinder (EXAKT 400CS, Norderstedt,

Germany) and stained using the von Kossa method. Transmitted light images of the stained sections were taken with an Olympus BX 50 microscope connected to a CCD camera (DP70, Olympus, Japan).

2.4.3 Histomorphometric analysis

Histomorphometric analysis was carried out using optical images of the stained sections and the ImageJ software (National Institutes of Health, USA). One section across the diameter of each defect was analyzed. The percent new bone formed in the defects was evaluated from the H&E stained sections. The entire defect area was determined as the area between the two defect margins, including the entire glass scaffold and the tissue within. The available pore area within the scaffold was determined by subtracting the area of the bioactive glass scaffold from the total defect area. The newly formed bone, fibrous tissue and bone marrow-like tissue within the defect area were then outlined and measured. The area of each tissue was expressed as a percentage of the available pore area of the scaffolds and total defect area.

The von Kossa-positive area in the defects implanted with the scaffolds was analyzed using the von Kossa stained sections and ImageJ. One section across the diameter of each defect was analyzed. Images were adjusted to measure only the black-stained areas of the image, which yielded the black area as a percentage of the total defect area. As mineralized bone and hydroxyapatite due to the glass conversion both bound the silver nitrate, in order to determine the percent area due to the conversion of the glass scaffold, the von Kossa-positive percentage was averaged for each sample and the percent new bone determined for each sample from the H&E stained images was subtracted.

Quantitation of blood vessels within the defect was performed using sections stained by the PAS technique, which results in purple-stained blood vessels with counterstaining yielding green-colored red blood cells. Viewed at 20x, each scaffold was scanned to acquire six regions of interest each within the fibrous tissue and new bone, and the blood vessels were outlined. All six areas were combined using ImageJ to determine the total blood vessel area, which was expressed as a percentage of the total area of the respective tissue (fibrous tissue or new bone).

2.5 Statistical analysis

All cell culture experiments (4 samples in each group) were run in triplicate. The data are presented as mean \pm SD. Analysis for differences between groups was performed using one-way ANOVA with Tukey's post hoc test. Differences were considered significant for $p < 0.05$. Statistical calculations were performed using the software package SigmaStat for Windows Version 2.03.

3. Results

3.1 Characteristics of as-fabricated scaffolds

The as-fabricated Cu-doped scaffolds (**Fig. 1a**) appeared blue, an indication that the Cu in the glass was present as Cu^{2+} ions, and the intensity of the blue color increased with the Cu concentration in the glass. The Cu dopant did not have any observable effect on the microstructure of the scaffolds, presumably because of the low Cu concentration in the glass and the use of a robocasting method to create the scaffolds which allowed precise control of the scaffold architecture. The scaffolds had a grid-like microstructure, composed of dense glass filaments (330 μm in diameter) and pores of size 300 μm in the plane of

deposition (xy plane) (**Fig.1b**) and 150 μm in the direction at right angles to the plane of deposition (z direction).

3.2 Degradation and conversion of scaffolds to hydroxyapatite in SBF

Immersion of the scaffolds in SBF resulted in the formation of a needle-like product on the surface of the glass filaments (**Fig. 1c**) which is typical of hydroxyapatite (HA) formed on the surface of bioactive glasses reacted in an aqueous phosphate solution [33]. Raman spectroscopy of the reacted scaffolds showed that the major resonance line corresponded to HA (**Fig. S1**).

Immersion of the scaffolds in SBF also resulted in a weight loss of the scaffolds (**Fig. 2a**) and an increase in pH of the solution (results not shown), as observed previously for 13-93 glass and other bioactive glasses [33]. The weight loss and pH curves of the four groups of scaffolds showed trends similar to those observed in previous studies [33]. A more rapid increase at earlier times (up to ~ 7 days) was followed by a slower increase thereafter and to a nearly constant value at longer times (longer than ~ 14 days). The Cu dopant concentrations used in the present study had no measurable effect on the weight loss of the 13-93 scaffolds. In addition, CuO dopant concentrations of 0.4 and 0.8 wt. % in the glass had no significant effect on the pH of the medium but the scaffolds doped with 2.0 wt. % CuO produced an increase in the pH. When the reaction was terminated at 28 days, the final weight loss and pH were $5.5 \pm 0.5\%$ and 7.80 ± 0.08 , respectively, which are consistent with previous results for the conversion of 13-93 glass in an aqueous phosphate solution [33, 35].

Figure 2b shows that the release of Cu ions from the glass into SBF was faster at earlier immersion times and it decreased continuously with time. At any immersion time, the cumulative amount of Cu ions released into the medium increased with increasing CuO in as-fabricated glass. When the experiments were terminated at 28 days, the total amount of Cu ions released was 2.3, 4.6, and 13.8 ppm, respectively, for the scaffolds doped with 0.4, 0.8 and 2.0 wt. % CuO.

3.3 Assessment of MC3T3-E1 cell proliferation and ALP activity in vitro

Quantitative measurement of MC3T3-E1 cell proliferation on the bioactive glass scaffolds showed a significant increase in cell number with incubation time for all four groups of scaffolds (**Fig. 3**). At each incubation time, the number of cells on the scaffolds doped with 0.4 and 0.8 wt. % CuO was not significantly different from the undoped scaffolds. In comparison, the cell number for the scaffolds doped with 2.0 wt. % CuO was significantly lower than the undoped 13-93 scaffolds, showing that the scaffolds doped with 2.0 wt. % CuO had a lower ability to support the proliferation of MC3T3-E1 cells.

The results of live cell/dead cell assays for MC3T3-E1 cells cultured on the four groups of scaffolds are shown in **Fig. 4**. The fluorochrome labeling of the cells cultured for up to 21 days on the 13-93 scaffolds and the 13-93 scaffolds doped with 0.4 or 0.8 wt. % CuO showed very few dead cells. The cells visible in the micrographs of these three groups were elongated and appeared to align along the long axis of the dense glass struts of the scaffold. The cells were well spread at all four culture intervals with numerous cytoplasmic projections and they appeared to be well attached to the surface of the glass. In comparison,

fewer live cells and a larger number of dead cells were found in the images for the 13-93 scaffolds doped with 2.0 wt. % CuO.

SEM images in **Fig. 5** show the morphology of MC3T3-E1 cells incubated on the surface of the four groups of scaffolds for 2, 7, and 14 days. The cells appeared to adhere to the surface of the scaffolds, presenting a well-spread morphology and maintaining their phenotype. The number of cells on the scaffolds increased with culture time. After an incubation time of 7 days, almost the whole surface of the scaffolds was covered with cells and cell spreading on the glass filaments was visible. The cells began to aggregate and the neighboring cells appeared to maintain physical contact with each other by multiple extensions. The cells incubated on the 13-93 scaffold and the 13-93 scaffold doped with 0.4 and 0.8 wt. % CuO grew into the pores of scaffolds and showed the formation of numerous cell projections, features that indicated firm cell attachment to the surface. While the cells grew on the surface of the 13-93 scaffolds doped with 2.0 wt. % CuO, they showed little tendency to infiltrate into the pores. In general, the results of the live cell/dead cell assays and the SEM images of the cell morphology were consistent with the results of the CCK-8 cell proliferation assays.

The results of spectrophotometric measurements of the ALP activity of MC3T3-E1 cells cultured on the four groups of scaffolds for 3, 7, and 14 days are presented in **Fig. 6**. The ALP activity increased significantly with incubation time for the cells cultured on the 13-93 scaffolds and the 13-93 scaffolds doped with 0.4 and 0.8 wt. % CuO, indicating that the cells were able to carry out an osteogenic function on these three groups of scaffolds. The significantly lower and almost constant ALP activity of the cells on the 13-93 scaffolds doped with 2.0 wt. % CuO indicated poor cytocompatibility for this scaffold group.

3.4 Assessment of new bone formation in rat calvarial defects in vivo

Transmitted light images of H&E stained sections of the rat calvarial defects implanted for 6 weeks with the four groups of scaffolds, as fabricated (without BMP2) or loaded with BMP2 (1 $\mu\text{g}/\text{defect}$), are shown in **Fig. 7**. For the as-fabricated scaffolds composed of 13-93 glass and 13-93 glass doped with 0.4 and 0.8 wt. % CuO, new bone infiltrated into the edges (periphery) adjacent to the host bone, indicating good integration of the scaffolds with the surrounding calvarial bone, and also formed islands within the pores of the scaffolds (**Fig. 7a1–c1**). Loading those three groups of scaffolds with BMP2 enhanced their capacity to regenerate bone considerably, with new bone almost completely infiltrating the pores of the scaffold and bridging the edges of the defect (**Fig. 7a2–c2**). In comparison, little new bone infiltrated the as-fabricated scaffolds composed of 13-93 glass doped with 2.0 wt. % CuO (**Fig. 7d1**). Loading those scaffolds with BMP2 improved their capacity to regenerate bone (**Fig. 7d2**). While new bone infiltrated the edges of the scaffold and also formed islands within the pores of the scaffold, the amount of new bone appeared to be significantly lower when compared to the other three groups of scaffolds.

Since all the scaffolds had the same microstructure, their capacity to regenerate bone in the defects was compared by normalizing the amount of new bone to the total pore space (area) of the scaffolds (**Fig. 8**). The amount of new bone in the defects implanted with the as-fabricated 13-93 bioactive glass scaffolds was $46 \pm 8\%$, a value that was comparable to those in previous studies [30, 36]. Doping the 13-93 glass with 0.4 or 0.8 wt. % CuO had no measurable effect on the capacity of the scaffolds to regenerate bone. The amount of new bone in the scaffolds doped with 0.4 wt. % CuO ($49 \pm 11\%$) and 0.8 wt. % CuO ($43 \pm 9\%$) was not significantly different from the 13-93 scaffolds. Loading

those three groups of scaffolds with BMP2 significantly enhanced their ability to regenerate bone. The enhancement found for the undoped 13-93 scaffolds was comparable to the results of a previous study [30]. In comparison, doping the 13-93 scaffolds with 2.0 wt. % CuO was significantly inhibited their capacity to regenerate bone (new bone = $0.8 \pm 0.7\%$). While the addition of BMP2 also improved the capacity of this scaffold group to regenerate bone, the amount of new bone was still significantly lower than the undoped 13-93 scaffolds without BMP2. These results indicate a significant capacity of the scaffolds doped with 2.0 wt. % CuO to inhibit bone regeneration and the ability of BMP2 to stimulate robust bone regeneration in all four groups of scaffolds.

3.5 Assessment of mineralized tissue and bioactive glass conversion

Transmitted light images of von Kossa stained sections of the rat calvarial defects implanted for 6 weeks with the four groups of bioactive glass scaffolds, as-fabricated or loaded with BMP2, are shown in **Fig. 9**. The von Kossa staining detects a combination of bone and glass converted to HA (or phosphate material). The total von Kossa-positive area, $39 \pm 6\%$, $41 \pm 7\%$ and $40 \pm 9\%$, respectively, for the defects implanted with the 13-93 scaffolds, 13-93 scaffolds doped with 0.4 wt. % CuO and 13-93 scaffolds doped with 0.8 wt. % CuO, showed no significant effect of the Cu doping (**Fig. 10a**). However, the total von Kossa-positive area for the defects implanted with the 13-93 scaffolds doped with 2.0 wt. % CuO ($18 \pm 5\%$) was significantly lower. Loading the scaffolds with BMP2 significantly enhanced the total von Kossa-positive area for all four groups of scaffolds. The von Kossa-positive area due to the glass conversion to HA showed no significant dependence on the amount of Cu doping used in this study (**Fig. 10b**). The results showed

an increase for all four groups of scaffolds loaded with BMP2 but the increase was not significant.

3.6 Assessment of fibrous tissue and marrow-like tissue

In addition to new bone infiltration, scaffolds implanted in the rat calvarial defects were infiltrated with fibrous (soft) tissue and marrow-like tissue. The results of the assessment of bone marrow-like and fibrous tissue in the four groups of scaffolds, as-fabricated or loaded with BMP2, are shown in **Fig. 11**. For the as-fabricated scaffolds, the pore space that was not infiltrated with new bone was filled mainly with fibrous tissue. In comparison, loading scaffolds with BMP2 reduced the amount of fibrous tissue but increased with amount of marrow-like tissue. The changes in fibrous and marrow-like tissue in all four groups of scaffolds due to the BMP2 loading were significant. In general, the results in **Fig. 11** show that when combined with BMP2 loading, doping the 13-93 scaffolds with increasing amount of Cu produced a decrease in marrow-like tissue and an increase in fibrous tissue.

3.7 Assessment of angiogenesis

Transmitted light images of PAS stained sections showed that blood vessels infiltrated the defects implanted with all four groups of scaffolds. As described earlier, in addition to the infiltration of new bone, the defects implanted with the as-fabricated scaffolds were also infiltrated with a considerable amount of fibrous tissue whereas the defects implanted with the BMP2-loaded scaffolds also contained a considerable amount of marrow-like tissue. Blood vessels were observed in the fibrous tissue while a

considerable amount of blood vessels was observed in the marrow-like tissue. Because the scaffolds doped with 2.0 wt. % CuO were infiltrated almost totally with fibrous tissue, the blood vessel area was evaluated separately in the fibrous tissue and in the new bone.

Figure 12 shows images of PAS stained sections of the defects implanted with the four groups of scaffolds at 6 weeks post-implantation. Sparse capillary vessels were observed in the fibrous tissue within the as-fabricated 13-93 scaffolds but a larger number of capillaries were found in the Cu-doped 13-93 scaffolds, particularly the scaffolds doped with 2.0 wt. % CuO. The percent blood vessel area in the defects implanted with the four groups of scaffolds, determined as a fraction of the total amount of fibrous tissue that infiltrated the scaffolds (**Fig. 13**), showed an increase in the average blood vessel area with increasing CuO in the glass. The scaffolds doped with 2.0 wt. % CuO had the highest blood vessel area within the fibrous tissue ($8 \pm 1\%$) which was significantly higher than the values for the as-fabricated 13-93 scaffolds ($4 \pm 1\%$), the scaffolds doped with 0.4 wt. % CuO ($5 \pm 1\%$) and the scaffolds doped with 0.8 wt. % CuO ($6 \pm 1\%$).

4. Discussion

Angiogenesis is essential for the healing of bone defects, particularly large (critical-size) defects. As the vasculature transports oxygen and nutrients to maintain healthy bone growth, the enhancement of angiogenesis should increase osteogenesis. Copper ions have been shown to play a direct role in stimulating angiogenesis [22, 23] and the delivery of Cu ions by borate-based bioactive glass scaffolds has been shown to enhance angiogenesis in subcutaneous sites and full thickness skin wounds in rodents [24, 25] and both angiogenesis and osteogenesis in rat calvarial defects [26]. In the present study, doping silicate 13-93 bioactive glass scaffolds with 0.4 and 0.8 wt. % CuO did not have a

significant effect on the response of MC3T3-E1 cells *in vitro* and on angiogenesis and osteogenesis in rat calvarial defects at 6 weeks postimplantation. In comparison, a dopant concentration of 2.0 wt. % CuO significantly enhanced angiogenesis in the fibrous tissue that infiltrated the scaffolds and significantly reduced osteogenesis. The addition of BMP2 (1 µg/defect) to the undoped or Cu-doped scaffolds significantly improved their ability to stimulate osteogenesis *in vivo*.

4.1 Release of Cu ions from scaffolds into SBF in vitro

Doping the parent 13-93 glass with 0.4–2.0 wt. % CuO did not have a significant effect on the degradation and conversion of the scaffolds to HA in SBF, as measured by the weight loss of the scaffolds. Cu ions generally function as a network modifier in the glass whereas the conversion reaction of the glass is dependent mainly on the chemical degradation of the glass network itself. As the glass degraded and converted to HA, Cu ions were released into the SBF. Consequently, the release profile of the Cu ions as a function of time showed a trend that was approximately similar to the weight loss of the scaffolds (**Fig. 1**). Whereas the release profile is dependent on the degradation and conversion rate of the glass, the amount of Cu ions released from the glass at any time scaled as the amount of CuO originally incorporated into the as-fabricated glass.

Theoretically, if all the Cu ions in glass dissolved into the medium, the concentration of Cu ions in the SBF would be 32, 64 and 160 ppm, respectively, for the scaffolds doped with 0.4, 0.8 and 2.0 wt. % CuO. The measured amount of Cu ions in the SBF when the experiments were terminated at 28 days was only 2.3, 4.6 and 13.8 ppm, respectively, for those three groups of scaffolds. The difference between the measured and

theoretical values could be accounted for in of the limited conversion of the 13-93 glass. Experimentally, the total weight loss of the three groups of scaffolds was 5.5 ± 0.5 wt. %. Assuming that the glass reacted completely and all the CaO in the glass reacted with phosphate ions from the medium to form HA, the theoretical weight loss would be 64%. If the Cu ions were released only from the fraction of the glass that reacted and converted to HA, the amount of Cu ions in the SBF is predicted to be 2.8, 5.5 and 13.7 ppm, respectively for the scaffolds doped with 0.4, 0.8 and 2.0 wt. % CuO. As these values are in good agreement with the measured values, the results indicate that Cu ions are released into the SBF almost exclusively from the reacted region of the glass.

4.2 Effect of Cu-doped scaffolds on MC3T3-E1 cell proliferation and function in vitro

The results of the present study showed that scaffolds of the parent (undoped) 13-93 glass supported the proliferation and ALP activity of preosteoblastic MC3T3-E1 cells *in vitro*, which is compatible with the results of previous studies using 13-93 glass in the form of porous or fibrous scaffolds and osteoblastic cells [34, 37]. Doping the 13-93 glass with 0.4 and 0.8 wt. % CuO did not change the ability of the scaffolds to support MC3T3-E1 cell proliferation on the surface and into the pores of the scaffolds (**Fig. 3, 5**). The ALP activity of the cells incubated for 7 and 14 days on the scaffolds doped with 0.4 and 0.8 wt. % CuO was higher than the cells cultured on the parent 13-93 scaffolds, indicating that the Cu ions could stimulate the ability of the cells to carry out an osteogenic function.

Doping the glass with 2.0 wt. % CuO significantly lowered the ability of the scaffolds to support the proliferation and ALP activity of the MC3T3-E1 cells. Live-cell/dead cell assays showed that the scaffolds doped with 2.0 wt. % CuO were toxic to the

cells (**Fig. 4**). The amount of Cu ions released from those scaffolds into the medium at day 1 was sufficient to cause a significant reduction in the number of MC3T3-E1 cells on those scaffolds. Thereafter, as the Cu ion release rate decreased with time, the cell number increased but it was still significantly lower than the undoped 13-93 scaffolds at each incubation time.

In the present study, the degradation of the scaffolds and release of ions were measured in SBF (1 g scaffold per 100 ml SBF) whereas the medium used in the cell culture experiments was α -MEM (1 scaffold of mass ~50 mg in 2 ml medium). A previous study showed approximately the same degradation rate of 13-93 glass in SBF and in Dulbecco's modified Eagle's medium (DMEM) for the same mass to volume ratio of glass to immersion medium [38]. Consequently, it can be assumed that for the same mass to volume ratio, the Cu ion release into α -MEM was approximately the same as in SBF. At day 1, the amount of Cu ions released from the scaffolds doped with 2.0 wt. % CuO into SBF was ~3 ppm. When compensated for the different mass to volume ratio, the amount of Cu ions released into the cell culture medium was ~7 ppm and ~10 ppm, respectively, at day 1 and day 2. Since the medium was replaced by fresh medium every 2 days, the concentration of Cu ions in the medium was highest and lowest, respectively, at the end of a two-day interval and at the beginning of the subsequent two-day interval. Furthermore, because the degradation rate of the glass decreased with time, the amount of Cu ions released into the medium during each successive two-day interval decreased with an increase in the total incubation time.

A previous study showed that scaffolds of a borate-based bioactive glass (porosity = 85%) doped with up to 3.0 wt. % CuO, with a much faster degradation rate than the 13-

93 glass used in the present study and, thus, a much faster Cu ion release rate, were not toxic to human bone marrow-derived stem cells (hBMSCs) *in vitro* [26]. The proliferation and ALP activity of hBMSCs incubated in the ionic dissolution product of silicate-based mesoporous bioactive glass that contained up to 5% Cu (molar fraction) did not show a significant dependence on the Cu content of the glass [39]. Mouse L929 fibroblasts, when incubated in the ionic dissolution product of Cu-containing intra-uterine devices, showed a decreasing viability with increasing Cu ion concentration in the range 0–100 ppm, reaching 50% viability and zero viability, respectively, when exposed to ~46 ppm and 100 ppm for 24 h [40].

Metals such as Ni, Co, Ag, Cu and Pd are common components of orthopedic and dental implants and the effects of their metal ion toxicity to cells *in vitro* have been widely studied. It is well established that above some threshold concentration, those metal ions are toxic to cells and that the threshold concentrations depends on both the composition of the metal and the cell line [41, 42]. Copper ions have been reported to catalyze the interaction between superoxide and hydrogen peroxide by the Haber-Weiss reaction, resulting in the reduction of Cu^{2+} to Cu^+ and the formation of toxic hydroxyl radicals [43]. Consequently, above a certain concentration, Cu ions can be toxic to cells due to the formation of an abundance of hydroxyl radicals.

In the present study, the toxicity of the scaffolds doped with 2.0 wt. % CuO appeared to result from a lower average Cu ion concentration in the medium when compared to the studies mentioned above. The difference may reside in a variety of factors. As described above, the threshold metal ion concentration for toxicity is known to depend on the cell line [42]. Another factor is the concentration gradient of the Cu ions in the

medium. Cells cultured in medium containing dissolved Cu ions experience a more uniform concentration of ions. In comparison, there is a gradient in Cu ion concentration when cells are incubated on the surface of a Cu-releasing bioactive glass scaffold, as done in the present study. The Cu ion concentration at the surface of the scaffold is typically much higher than the average concentration of the medium. In the present study, although the average Cu ion concentration in the medium was ~7 and 10 ppm, respectively, at days 1 and 2, the concentration was expected to be considerably higher at the surface of the scaffolds in contact with the cells and within the pores of the scaffolds. The composition of the glass scaffold can also have an effect on the threshold Cu ion concentration for toxicity because other ions such as Ca, Na, K, B and Si can be released (depending on the glass composition) and there is typically an increase in pH of the medium.

4.3 Effect of Cu-doped scaffolds on bone regeneration and angiogenesis in vivo

Bone regeneration at 6 weeks in rat calvarial defects implanted with the four groups of scaffolds showed trends similar to the MC3T3-E1 cell proliferation results described above. Doping the parent 13-93 glass with 0.4 and 0.8 wt. % CuO did not affect the capacity of the scaffolds to regenerate bone (**Fig. 8**). In comparison, bone regeneration in the defects implanted with the scaffolds doped with 2.0 wt. % was significantly inhibited and the amount of new bone was almost negligible ($0.8 \pm 0.7\%$ of the available pore volume). The lack of ability to support new bone infiltration by these scaffolds is presumably related to a high concentration of Cu ions at the surface (periphery) of the scaffolds and within the pores of the scaffolds (discussed above) which was presumably toxic to osteoblastic cells *in vitro*.

As bone regeneration in the defects implanted with scaffolds of 13-93 glass doped with 2.0 wt. % CuO was very limited, the formation of blood vessels was evaluated separately in the new bone and in the fibrous tissue that infiltrated the pores of the scaffolds [Fig. 13]. The blood vessel area in the new bone was not affected by doping the parent 13-93 glass with 0.4 and 0.8 wt. % CuO. In comparison, the blood vessel area in the fibrous tissue increased with increasing CuO in the glass. The blood vessel area in the fibrous tissue that infiltrated the scaffolds doped with 2.0 wt. % CuO was significantly higher than the parent 13-93 scaffolds, with a value that was approximately twice that for the parent 13-93 scaffolds.

The significant increase in blood vessel area in the soft tissue that infiltrated the scaffolds doped with 2.0 wt. % CuO is compatible with the observations of previous studies which showed the capacity of Cu ion release from borate-based bioactive glass and calcium phosphate-based scaffolds to enhance angiogenesis in animal models of soft tissue repair. Fibrous scaffolds of a borate bioactive glass doped with 0.1–2.0 wt. % CuO were found to be biocompatible while the scaffolds doped with 0.4 wt. % CuO significantly enhanced blood vessel formation in rat subcutaneous sites at 6 weeks post-implantation [44]. Copper ion release from calcium phosphate-based scaffolds was found to enhance angiogenesis in the peritoneal cavity of mice [21].

The effect of Cu ion release from borate-based bioactive glass scaffolds on bone regeneration and angiogenesis in osseous defects has been investigated in a rodent model. The borate-based bioactive glass had a much faster degradation and conversion rate to HA. In one study, borate bioactive glass doped with 0.4 wt. % CuO were formed into different porous architectures, referred to as trabecular, oriented and fibrous, and implanted for 12

weeks in rat calvarial defects. The Cu doping had no significant effect on bone regeneration and blood vessel area in the defects implanted with the trabecular and oriented scaffolds but it enhanced bone regeneration by the fibrous scaffolds [45]. A recent study found that a borate-based bioactive glass doped with 3.0 wt. % CuO enhanced both blood vessel formation and bone regeneration in rat calvarial defects at 8 weeks postimplantation [26].

While important, angiogenesis is a transitory event in bone regeneration, typically more prominent at an earlier stage of defect healing. Presumably the angiogenesis event had considerably diminished by the six-week implantation time used in the present study. However, doping the 13-93 glass with 0.4 and 0.8 wt. % CuO had no significant effect on bone regeneration at 6 weeks postimplantation.

Loading scaffolds composed of the parent 13-93 glass with BMP2 (1 $\mu\text{g}/\text{defect}$), significantly enhanced bone regeneration in the rat calvarial defects at 6 weeks postimplantation (**Fig. 8**), in agreement with the results of recent studies [30, 36]. Loading the 13-93 scaffolds doped with 0.4 and 0.8 wt. % CuO also enhanced bone regeneration significantly but the enhancement was comparable to the 13-93 scaffolds. The combination of BMP2 loading and Cu doping produced no significant benefit over the BMP2 loading alone, indicating no synergistic effects between the BMP2 loading and the Cu doping at the concentrations used in the present study. Although there are concerns about the safety of supra-physiological doses of BMP2 *in vivo*, loading silicate-based bioactive glass scaffolds with clinically safe doses of BMP2 appears to considerably more effective than Cu doping in regenerating sufficient bone within a clinically relevant time.

5. Conclusion

Scaffolds with a grid-like microstructure composed of silicate 13-93 bioactive glass doped with varying amounts of Cu (0-2.0 wt. % CuO) were created by robotic deposition and evaluated *in vitro* and *in vivo*. When immersed in simulated body fluid (SBF), the scaffolds released Cu ions in a dose-dependent manner but the Cu doping had no significant effect on the degradation and conversion of the scaffolds to hydroxyapatite. CuO dopant concentrations of 0.4 and 0.8 wt. % had no significant effect on the number and alkaline phosphatase activity of MC3T3-E1 cells cultured on the scaffolds *in vitro* and on bone regeneration and angiogenesis in rat calvarial defects at 6 weeks postimplantation. CuO dopant concentration of 2.0 wt. % significantly reduced the number and ALP activity of MC3T3-E1 cells *in vitro* and bone regeneration *in vivo* but significantly enhanced blood vessel area in the fibrous tissue that infiltrated the scaffolds. Loading the undoped or Cu-doped scaffolds with BMP2 (1 $\mu\text{g}/\text{defect}$) significantly enhanced their capacity to regenerate bone. Doping 13-93 bioactive glass scaffolds with 0.4 and 0.8 wt. % CuO had no significant effect on the response of MC3T3-E1 cells *in vitro* and bone regeneration in rat calvarial defects *in vivo* but a CuO concentration of 2.0 wt. % was toxic to the MC3T3-E1 cells and severely inhibited bone regeneration.

References

- [1] Giannoudis PV, Dinopoulos H, Tsiridis E. Bone substitutes: an update. *Injury* 2005;36S:S20–37.
- [2] Laurencin C, Khan Y, El-Amin SF. Bone graft substitutes. *Expert Rev Med Devices* 2006;3:49–57.
- [3] Hutmacher DW. Scaffolds in tissue engineering bone and cartilage. *Biomaterials* 2000;21:2529–43.

- [4] Karageorgiou V, Kaplan D. Potential of 3D biomaterial scaffolds and osteogenesis. *Biomaterials* 2005;26:5474–91.
- [5] Rickert D, Slater JJ, Meijer HJ, Vissink A, Raghoobar GM. Maxillary sinus lift with solely autogenous bone compared to a combination of autogenous bone and growth factors or (solely) bone substitutes. A systematic review. *Int J Oral Max Surg* 2012;41:160–7.
- [6] Tadjedin ES, de Lange GL, Lyaruu DM, Kuiper L, Burger EH. High concentrations of bioactive glass material (BioGran) vs. autogenous bone for sinus floor elevation. *Clin Oral Implan Res* 2002;13:428–36.
- [7] Wikesjo UM, Qahash M, Huang YH, Xiropaidis A, Polimeni G, Susin C. Bone morphogenetic proteins for periodontal and alveolar indications; biological observations - clinical implications. *Orthod Craniofac Res* 2009;12:263–70.
- [8] Polo CI, Oliveira Lima JL, De Lucca L, Piacuzzi CB, Naclerio-Homem MD, Arana-Chavez VE, et al. Effect of recombinant human bone morphogenetic protein 2 associated with a variety of bone substitutes on vertical guided bone regeneration in rabbit calvarium. *J Periodontol* 2013;84:360–70.
- [9] Zheng LW, Wong MC, Rabie AB, Cheung LK. Evaluation of recombinant human bone morphogenetic protein-2 in mandibular distraction osteogenesis in rabbits: Effect of dosage and number of doses on formation of bone. *Brit J Oral Max Surg* 2006;44:487–94.
- [10] Carragee EJ, Hurwitz EL, Weiner BK. A critical review of recombinant human bone morphogenetic protein-2 trials in spinal surgery: emerging safety concerns and lessons learned. *Spine J* 2011;11:471–91.
- [11] Williams BJ, Smith JS, Fu KM, Hamilton DK, Polly DW, Jr., Ames CP, et al. Does bone morphogenetic protein increase the incidence of perioperative complications in spinal fusion? A comparison of 55,862 cases of spinal fusion with and without bone morphogenetic protein. *Spine* 2011;36:1685–91.
- [12] Fang TD, Salim A, Xia W, Nacamuli RP, Guccione S, Song HM, Carano RA, Filvaroff EH, Bednarski MD, Giaccia AJ, Longaker MT. Angiogenesis is required for successful bone induction during distraction osteogenesis. *J Bone Miner Res* 2005;20:1114–24.
- [13] Kanczler JM, Oreffo ROC. Osteogenesis and angiogenesis: The potential for engineering bone. *Eur Cells Mater* 2008;15:100–14.
- [14] Kaigler JM, Wang D, Horger K, Mooney DJ, Kresbach PH. VEGF scaffolds enhance angiogenesis and bone regeneration in irradiated osseous defects. *J Bone Miner Res* 2006;21:735–44.

- [15] Nomi M, Atala A, Coppi PD, Soker S. Principals of neovascularization for tissue engineering. *Mol Asp Med* 2002;23:463–83.
- [16] Madeddu P. Therapeutic angiogenesis and vasculogenesis for tissue regeneration. *Exp Physiol* 2005;90:315–26.
- [17] Hanft JR, Pollak RA, Barbul A, van Gils C, Kwon PS, Gray SM, et al. Phase I trial on the safety of topical rhVEGF on chronic neuropathic diabetic foot ulcers. *J Wound Care* 2008;17:30–2, 34–7.
- [18] Uchi H, Igarashi A, Urabe K, Koga T, Nakayama J, Kawamori R, et al. Clinical efficacy of basic fibroblast growth factor (bFGF) for diabetic ulcer. *Eur J Dermatol* 2009;19:461–8.
- [19] Gerard C, Bordeleau LJ, Barralet J, Doillon CJ. The stimulation of angiogenesis and collagen deposition by copper. *Biomaterials* 2010;31:824–31.
- [20] Finney L, Vogt S, Fukai T, Glesne D. Copper and angiogenesis: unravelling a relationship key to cancer progression. *Clin Exp Pharmacol Physiol* 2009;36:88–94.
- [21] Barralet J, Gbureck U, Hbibovic P, Vorndran E, Gerard C, Doillon CJ. Angiogenesis in calcium phosphate scaffolds by inorganic copper ion release. *Tissue Eng Part A* 2009;15:1601–9.
- [22] Sen CK, Khanna S, Venojarvi M, Trikha P, Ellison EC, Hunt TK. Copper-induced vascular endothelial growth factor expression and wound healing. *Amer J Physiol Heart Circ Physiol* 2002;282:1821–27.
- [23] Frangoulis M, Georgiou P, Chrisostomidis C, Perrea D, Dontas I, Kavantzias N. Rat epigastric flap survival and VEGF expression after local copper application. *Plast Reconstr Surg* 2007;119:837–43.
- [24] Lin Y, Brown RF, Jung SB, Day DE. Angiogenic effects of borate glass microfibers in a rodent model. *J Biomed Mater Res A* 2014;102:4491–99.
- [25] Zhao S, Li L, Wang H, Zhang Y, Cheng X, Zhou N, Rahaman MN, Liu Z, Huang W, Zhang C. Wound dressings composed of copper-doped borate bioactive glass microfibers stimulate angiogenesis and heal full-thickness skin defects in a rodent model. *Biomaterials* 2015;53:379–91.
- [26] Zhao S, Wang H, Zhang Y, Huang W, Rahaman MN, Liu Z, Wang D, Zhang C. Copper-doped borosilicate bioactive glass scaffolds with improved angiogenic and osteogenic capacity for repairing osseous defects. *Acta Biomater* 2015;14:185–96.

- [27] Rahaman MN, Day DE, Bal BS, Fu Q, Jung SB, Bonewald LF, Tomsia AP. Bioactive glass in tissue engineering. *Acta Biomater* 2011;7:2355–73.
- [28] Jones JR. Review of bioactive glass: From Hench to hybrids. *Acta Biomater* 2013;9:4457–86.
- [29] Liu X, Rahaman MN, Hilmas GE, Bal BS. Mechanical properties of bioactive glass (13-93) scaffolds fabricated by robotic deposition for structural bone repair. *Acta Biomater* 2013;9:7025-34.
- [30] Liu X, Rahaman MN, Liu Y, Bal BS, Bonewald LF. Enhanced bone regeneration in rat calvarial defects implanted with surface-modified and BMP-loaded bioactive glass (13-93) scaffolds. *Acta Biomater* 2013;9:7506-17.
- [31] Kokubo T, Kushitani H, Sakka S, Kitsugi T, Yamamuro T. Solutions able to reproduce *in vivo* surface-structure changes in bioactive glass-ceramic A-W. *J Biomed Mater Res* 1990;24:721–34.
- [32] Huang W, Rahaman MN, Day DE, Li Y. Mechanisms of converting silicate, borate, and borosilicate glasses to hydroxyapatite in dilute phosphate solutions. *Phys Chem Glasses B* 2006;47:647–58.
- [33] Fu Q, Rahaman MN, Fu H, Liu X. Silicate, borosilicate, and borate bioactive glass scaffolds with controllable degradation rate for bone tissue engineering applications. I. Preparation and *in vitro* degradation. *J Biomed Mater Res A* 2010; 95:164–71.
- [34] Brown RF, Day DE, Day TE, Jung S, Rahaman MN, Fu Q. Growth and differentiation of osteoblastic cells on 13-93 bioactive glass fibers and scaffolds. *Acta Biomater* 2008;4:387 – 96.
- [35] Yao A, Wang D, Huang W, Rahaman MN, Day DE. *In vitro* bioactive characteristics of borate-based glasses with controllable degradation behavior. *J Am Ceram Soc* 2007;90:303–6.
- [36] Lin Y, Xiao W, Liu X, Bal BS, Bonewald LF, Rahaman MN. Long-term bone regeneration, mineralization and angiogenesis in rat calvarial defects implanted with strong porous bioactive glass (13-93) scaffolds. *J Non-Cryst Solids* 2015; in press. <http://dx.doi.org/10.1016/j.noncrsol.2015.04.008>.
- [37] Fu Q, Rahaman MN, Bal BS, Brown RF, Day DE. Mechanical and *in vitro* performance of 13–93 bioactive glass scaffolds prepared by a polymer foam replication technique. *Acta Biomater* 2008;4:1854–64.

- [38] Gu Y, Huang W, Rahaman MN. Effect of immersion medium on the degradation and conversion of 13-93 bioactive glass *in vitro*. Ceramic Transactions, Proceedings of MS&T 14; in press.
- [39] Wu C, Zhou Y, Xu M, Han P, Chen L, Chang J, Xiao Y. Copper-containing mesoporous bioactive glass scaffolds with multifunctional properties of angiogenesis capacity, osteostimulation and antibacterial activity. Biomaterials 2013;34:422–33.
- [40] Cao B, Zheng Y, Xi T, Zhang C, Song W, Burugapalli K, Yang H, Ma Y. Concentration-dependent cytotoxicity of copper ions on mouse fibroblasts *in vitro*: effects of copper ion release from TCu380A vs TCu220C intra-uterine devices. Biomed Microdevices 2012;14:709–20.
- [41] Wataha JC, Hanks CT, Craig RG. The *in vitro* effects of metal cations on eukaryotic cell metabolism. J Biomed Mater Res 1991;25:1133–49.
- [42] Wataha JC, Hanks CT, Sun Z. Effect of cell line on *in vitro* metal ion cytotoxicity. Dent Mater 1994;10:156–61.
- [43] Ueda J, Takai M, Shimazu Y, Ozawa T. Reactive oxygen species generated from the reaction of copper(II) complexes with biological reductants cause DNA strand scission. Arch Biochem Biophys 1998;357:231–9.
- [44] Jung SB. Bioactive borate glasses. Bio-glasses: an introduction. 2012. p. 75–95.
- [45] Bi L, Rahaman MN, Day DE, Brown Z, Samujh C, Liu X, Mohammadkhah A, Dusevich V, Eick JD, Bonewald LF. Effect of borate bioactive glass microstructure on bone regeneration, angiogenesis, and hydroxyapatite conversion in a rat calvarial defect model. Acta Biomater 2013;9:8015–26.

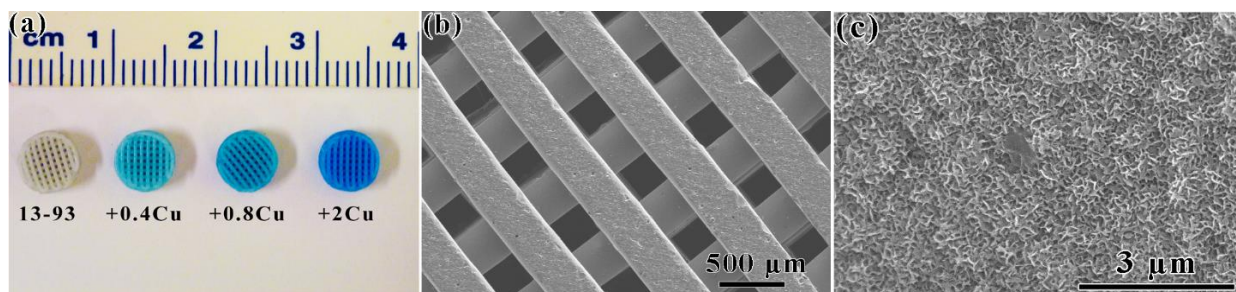


Fig. 1. (a) Optical image of the four groups of as-fabricated scaffolds prepared by robocasting, composed of (left to right) 13-93 glass and 13-93 glass doped with 0.4, 0.8 and 2.0 wt. % CuO; (b) SEM image of the top surface of a 13-93 scaffold doped with 0.8 wt. % CuO; (c) SEM image of the surface of a glass filament (0.8 wt. % CuO) after immersion of the scaffold in SBF at 37 °C for 7 days.

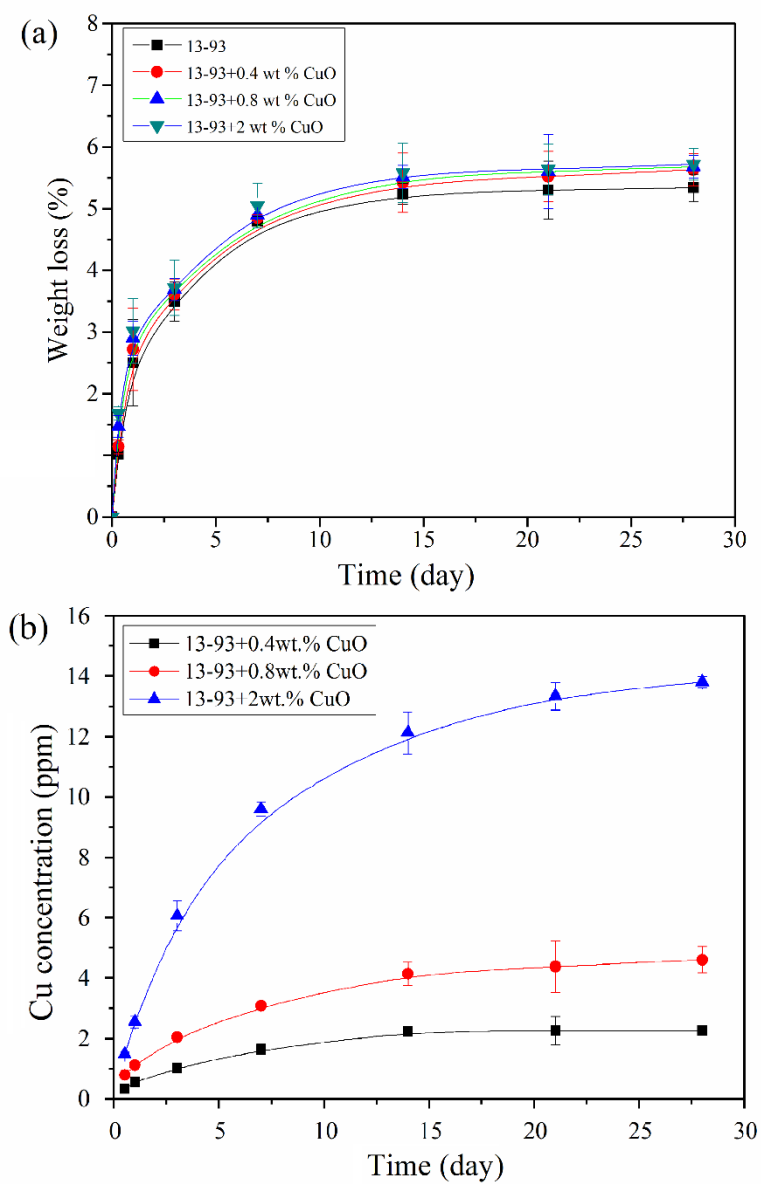


Fig. 2. (a) Weight loss of 13-93 scaffolds and scaffolds doped with 0.4, 0.8 and 2.0 wt. % CuO and (b) cumulative amount of Cu ions released from 13-93 scaffolds doped with 0.4, 0.8 and 2.0 wt. % CuO as a function of immersion time in SBF.

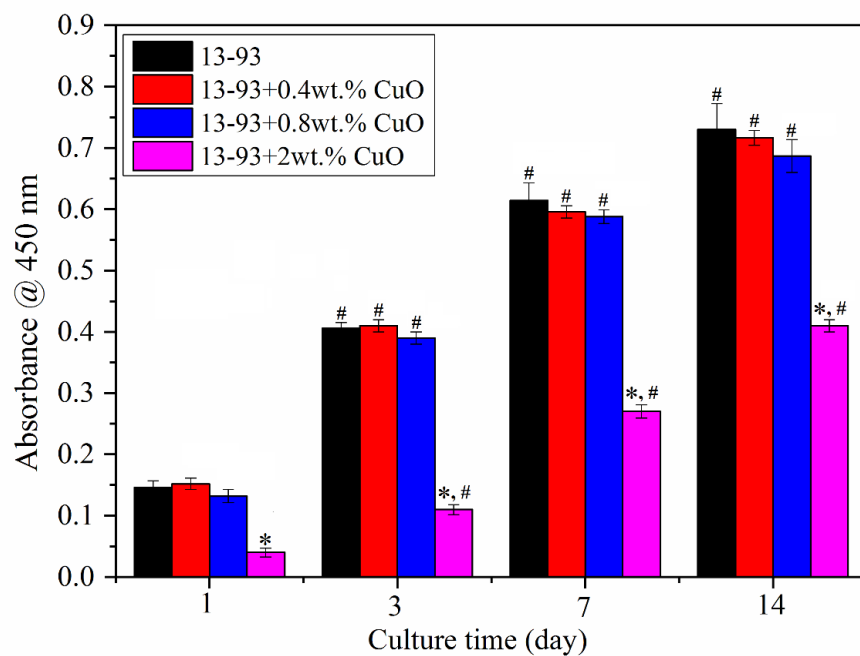


Fig. 3. Cell proliferation, as measured by CCK-8 assay, of MC3T3-E1 cells cultured on the four groups of bioactive glass scaffolds for the times shown. (Average \pm SD, $n = 3$; *significant difference when compared to 13-93 scaffold at the same incubation time; #significant difference when compared to same group at different incubation times, $p < 0.05$)

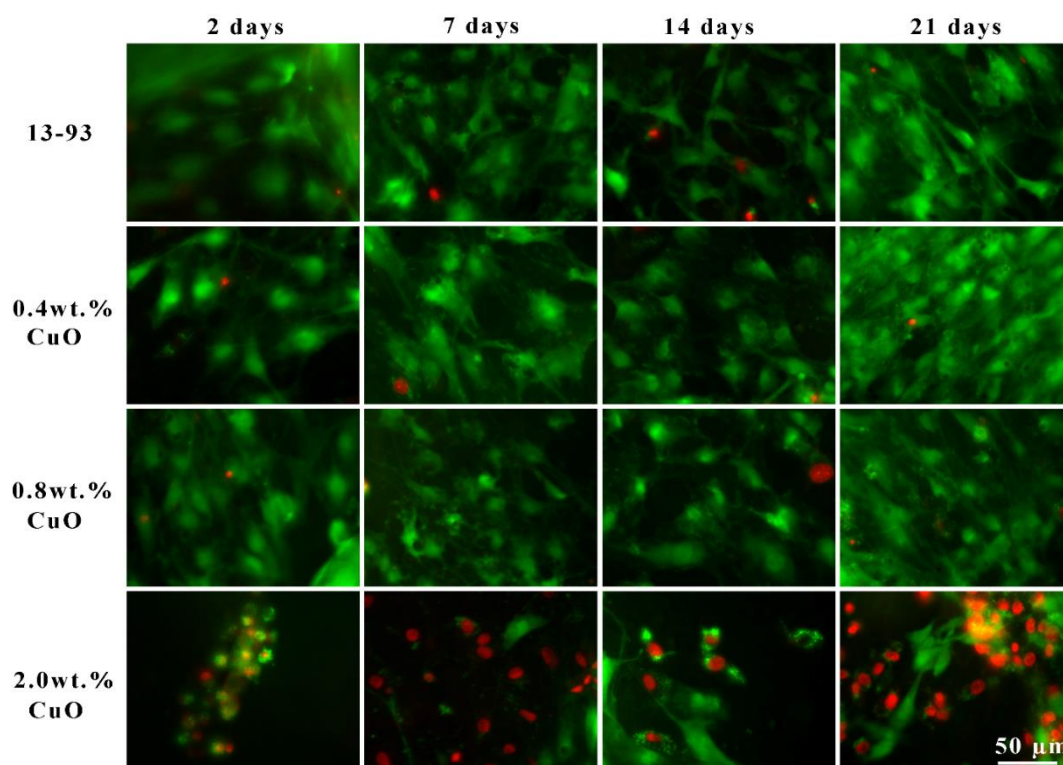


Fig. 4. Fluorescent images of MC3T3-E1 cells incubated for 2, 7, 14 and 21 days on the four groups of bioactive glass scaffolds. Double staining was used to detect live cells as green fluorescent and dead cells as red fluorescent.

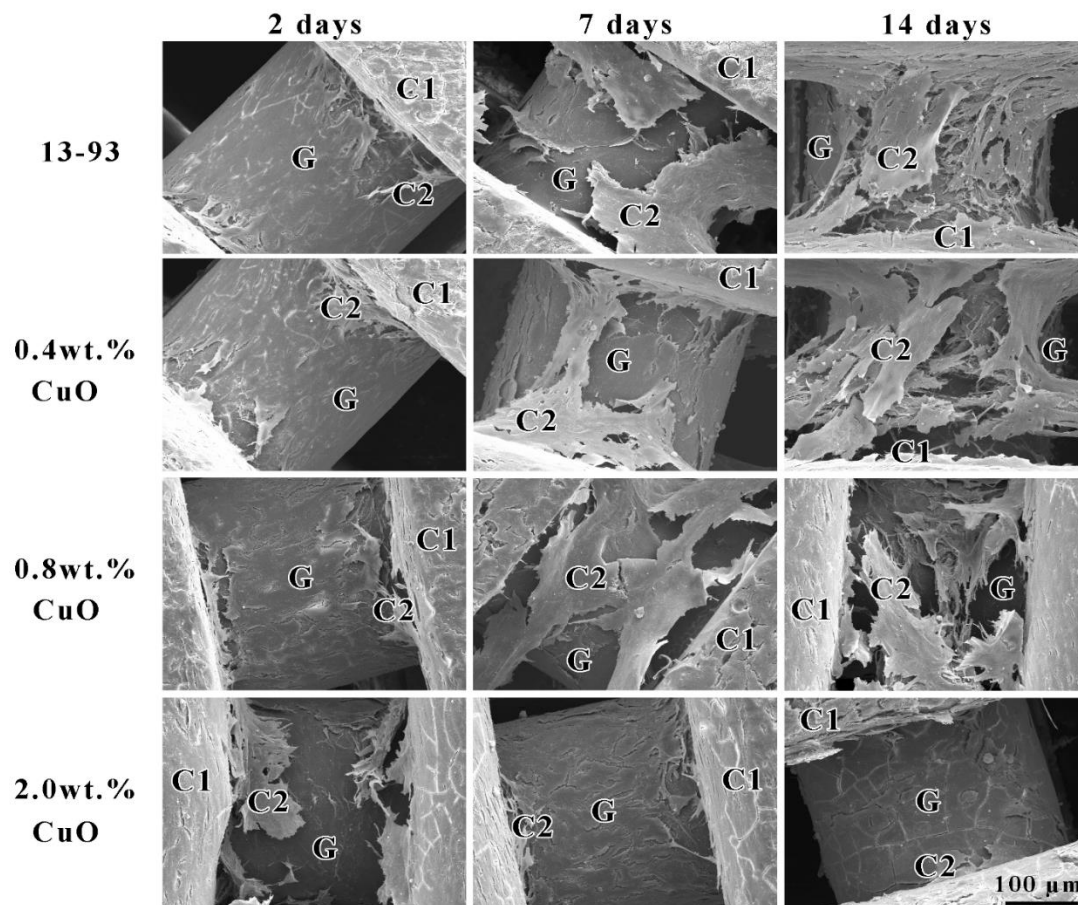


Fig. 5. SEM images of the four groups of bioactive glass scaffolds seeded with MC3T3-E1 cells and incubated for 2, 7 and 14 days. (C1: cells on surface filaments; C2: cells on filaments below the surface; G: bioactive glass filament below surface.)

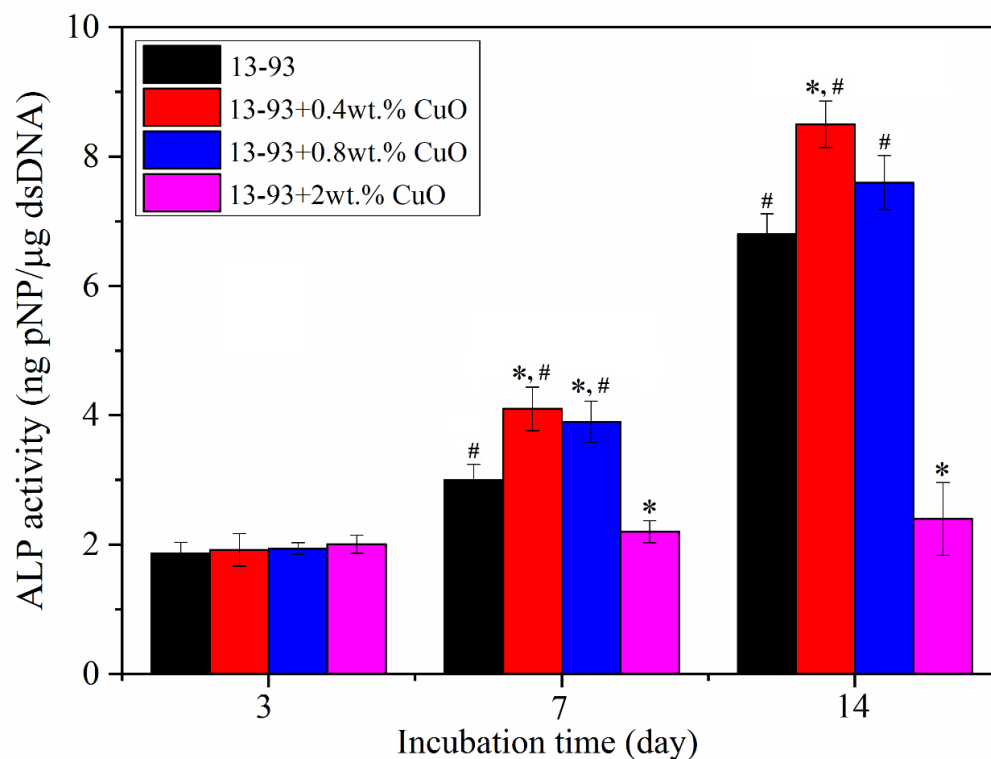


Fig. 6. Alkaline phosphatase (ALP) activity of MC3T3-E1 cells cultured on 13-93 scaffolds and on 13-93 scaffolds doped with 0.4, 0.8 and 2.0 wt. % CuO for the times shown. Enzyme activity is expressed as ng of pNP formed per μg dsDNA per 30 min. (Average \pm SD, $n = 3$; *significant difference when compared to 13-93 scaffold at the same incubation time; #significant difference when compared to same group at different incubation times; $p < 0.05$).

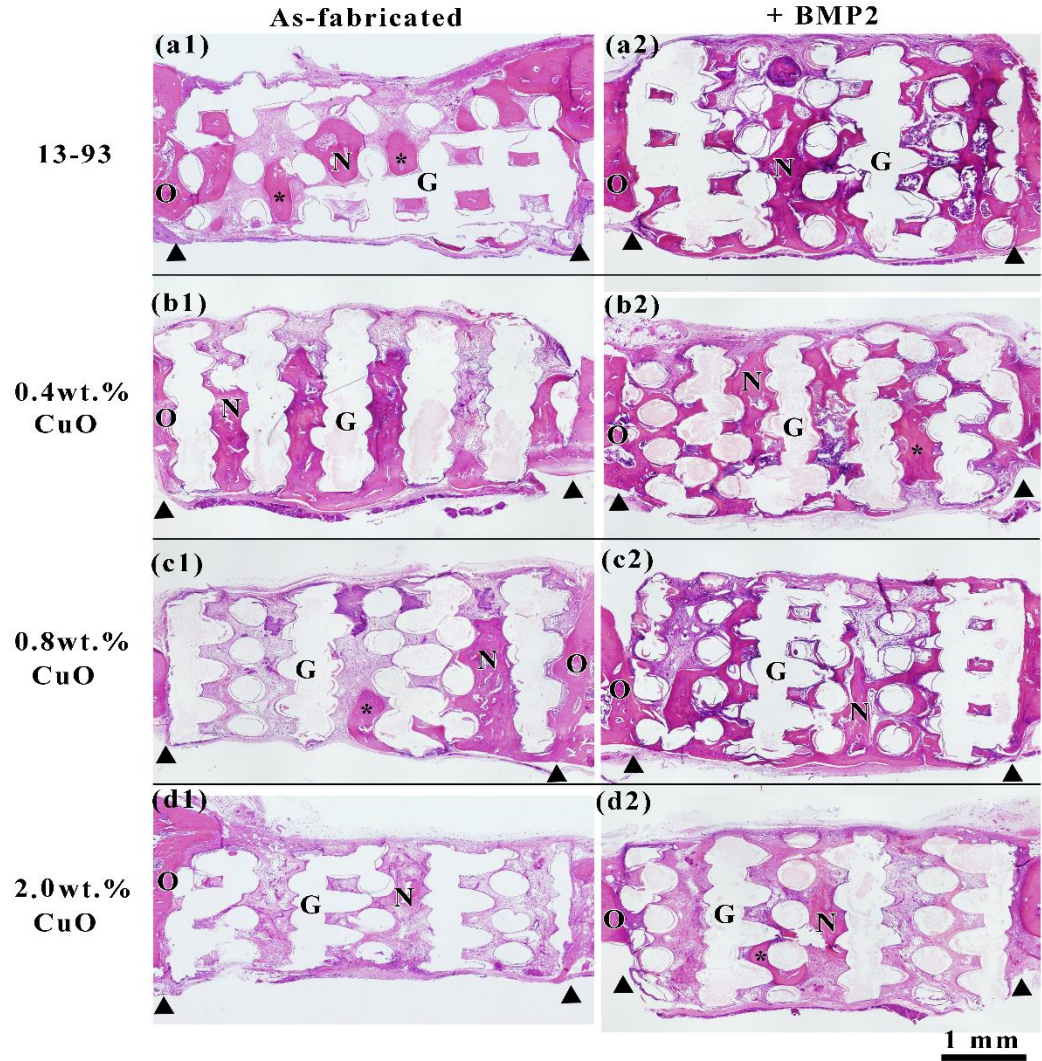


Fig. 7. Transmitted light images of H&E-stained sections of rat calvarial defects implanted with the four groups of bioactive glass scaffolds, as fabricated (left) or loaded with BMP2 (right), at 6 weeks postimplantation. N = new bone; O = host bone; * = bony island; G = bioactive glass; arrowheads indicate the edges of host bone.

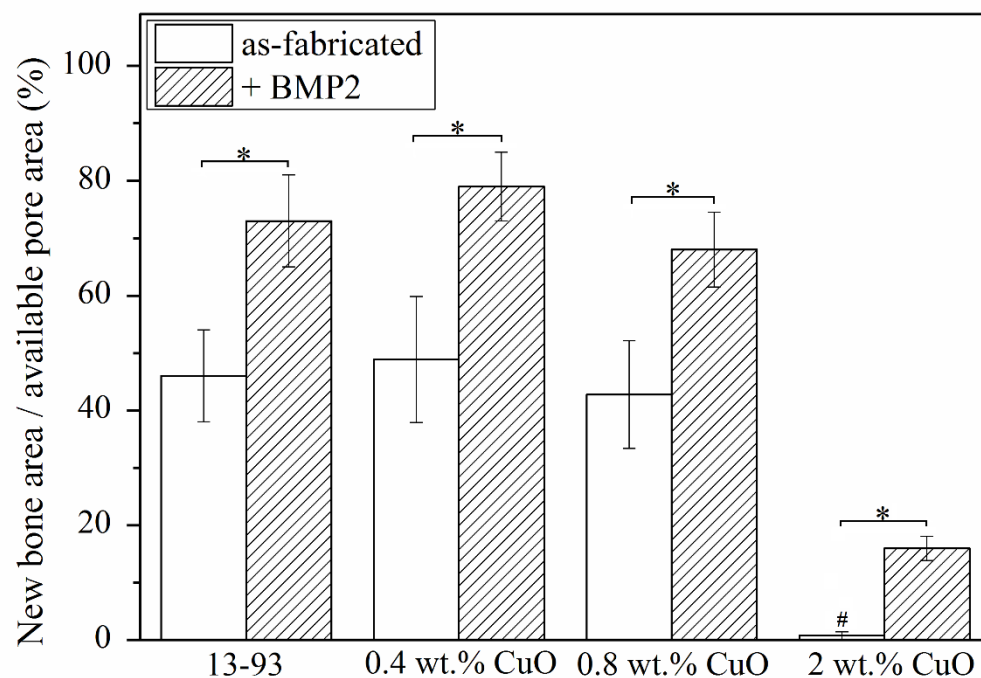


Fig. 8. Percent new bone in rat calvarial defects implanted with the four groups of scaffolds, 13-93 and 13-93 doped with 0.4, 0.8 and 2.0 wt. % CuO, as-fabricated or loaded with BMP2, at 6 weeks postimplantation. The amount of new bone is shown as a percent of the available pore space (area) of the scaffolds. (*significant difference between groups; #significant difference when compared to as-fabricated 13-93 scaffolds; $p < 0.05$)

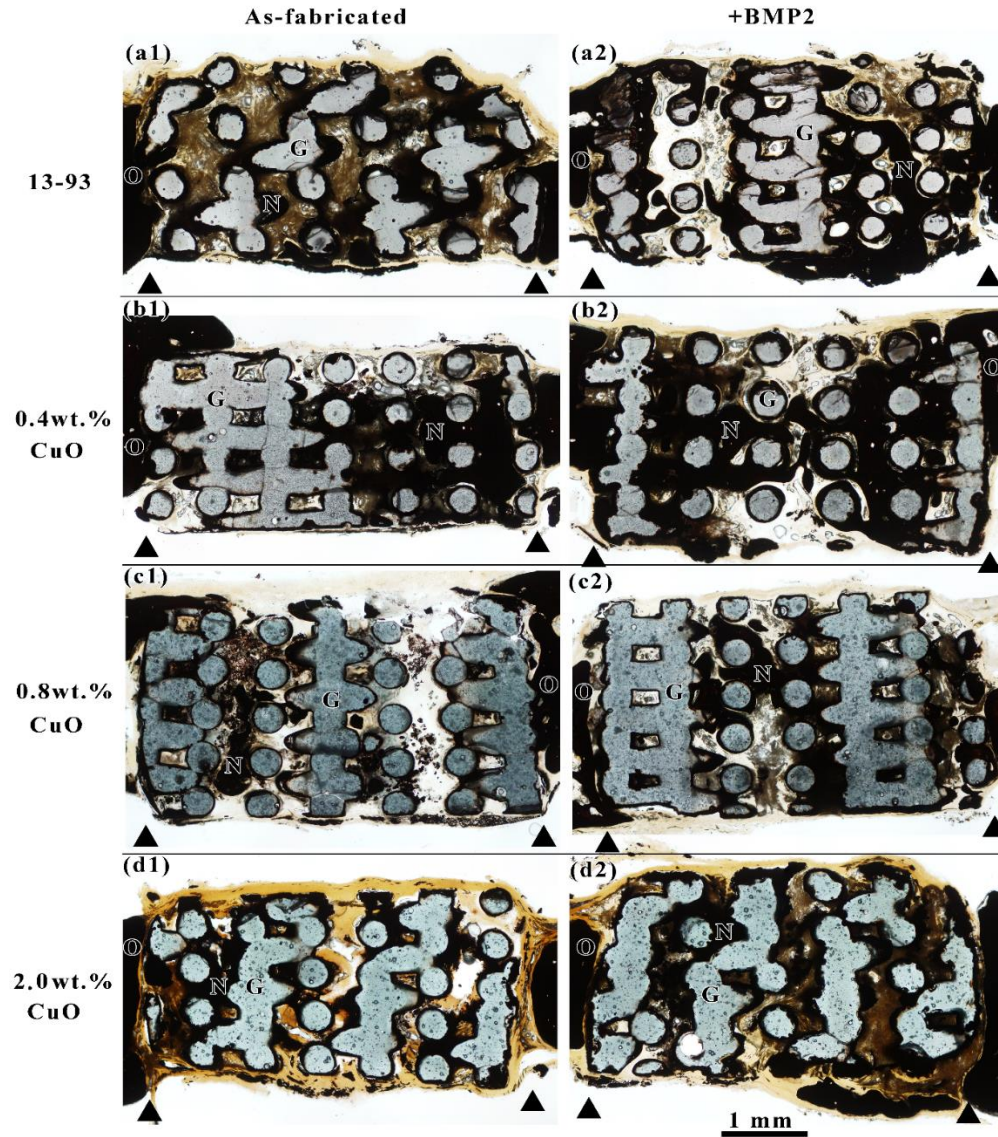


Fig. 9. Transmitted light images of von Kossa stained sections of rat calvarial defects implanted with the four groups of scaffolds, as-fabricated (left) or loaded with BMP2 (right), at 6 weeks postimplantation. N = new bone; O = host bone; G = bioactive glass; arrowheads indicate the edges of host bone.

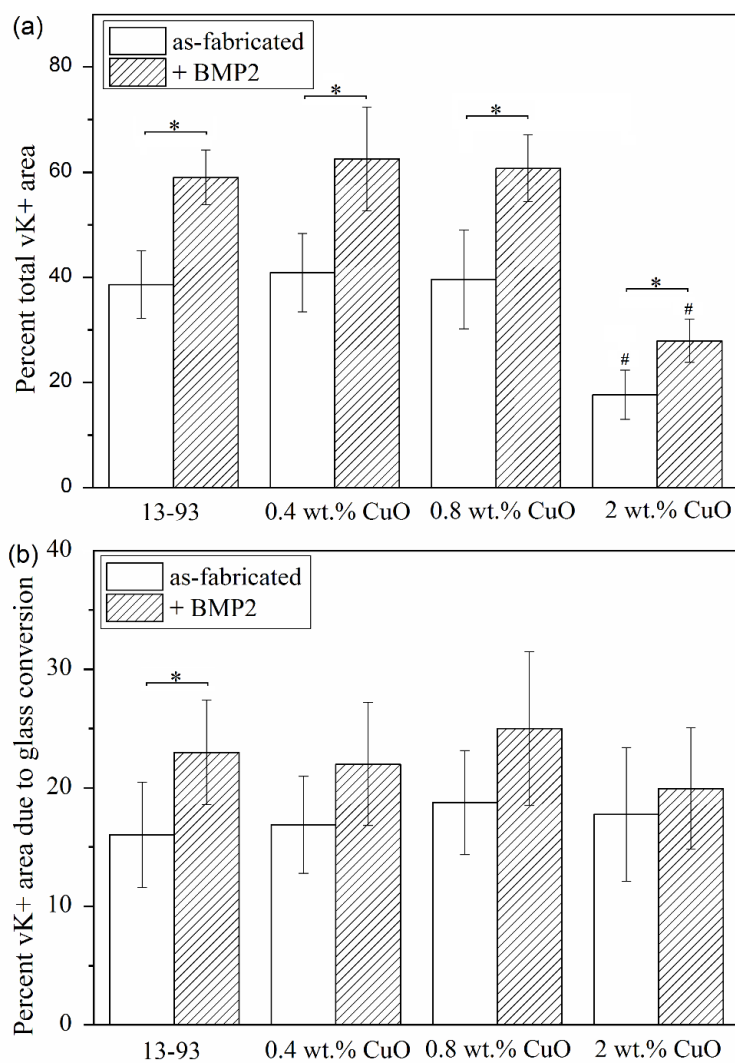


Fig. 10. Percent total von Kossa positive (vK+) area (a) and vK+ area due to the bioactive glass conversion (b), determined as a fraction of the total defect area, for rat calvarial defects implanted with the four groups of scaffolds, as fabricated or loaded with BMP2, at 6 weeks post-implantation. (average \pm SD; *significant difference between groups; #significant difference when compared to the same 13-93 scaffold group; $p < 0.05$)

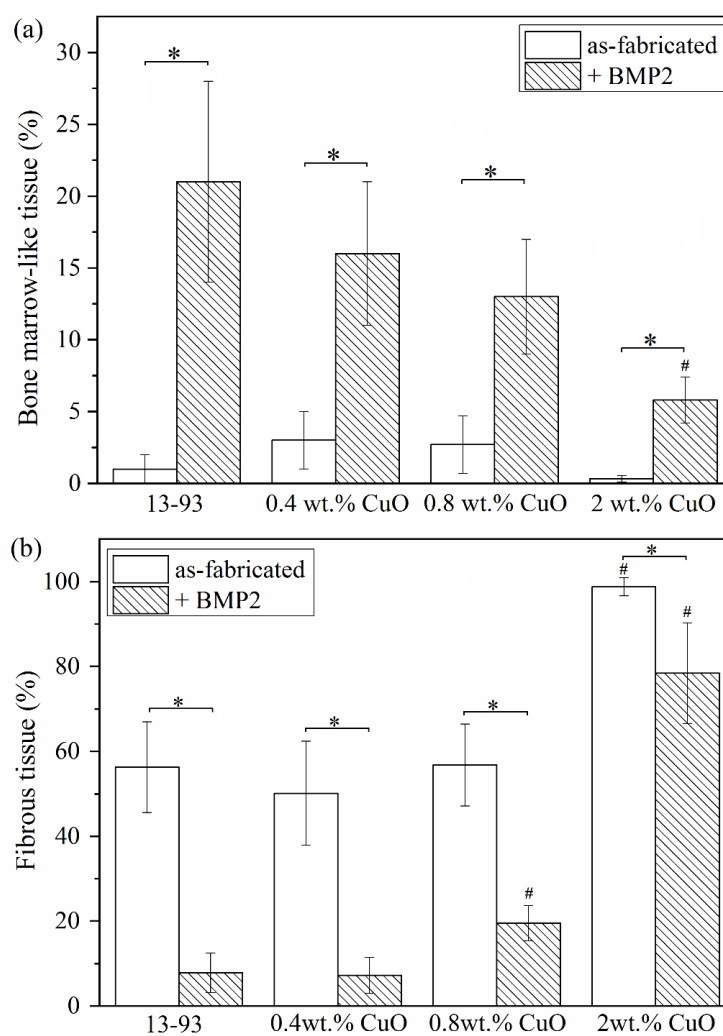


Fig. 11. Percent bone marrow-like tissue (a) and fibrous tissue (b) in rat calvarial defects implanted with the four groups of scaffolds, as fabricated or loaded with BMP2, at 6 weeks post-implantation (*significant difference between groups; #significant difference when compared to the same 13-93 scaffold group; $p < 0.05$)

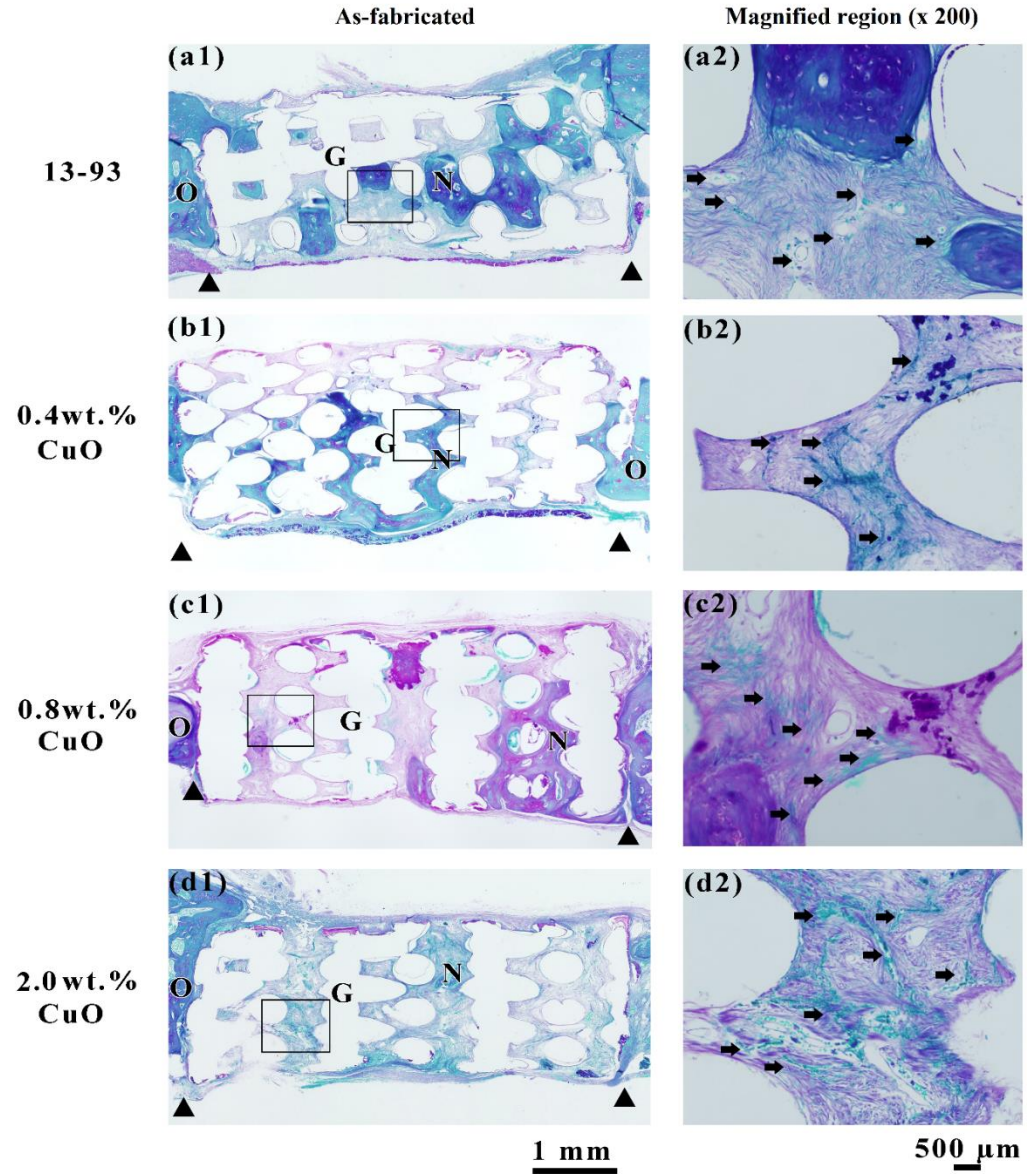


Fig. 12. (Left): Transmitted light images of PAS stained sections of rat calvarial defects implanted with the four groups of scaffolds (without BMP2) at 6 weeks postimplantation; (Right): magnified images of the boxed areas in the corresponding images on the left. (N = new bone; G = bioactive glass; Arrows indicate some of the blood vessels.)

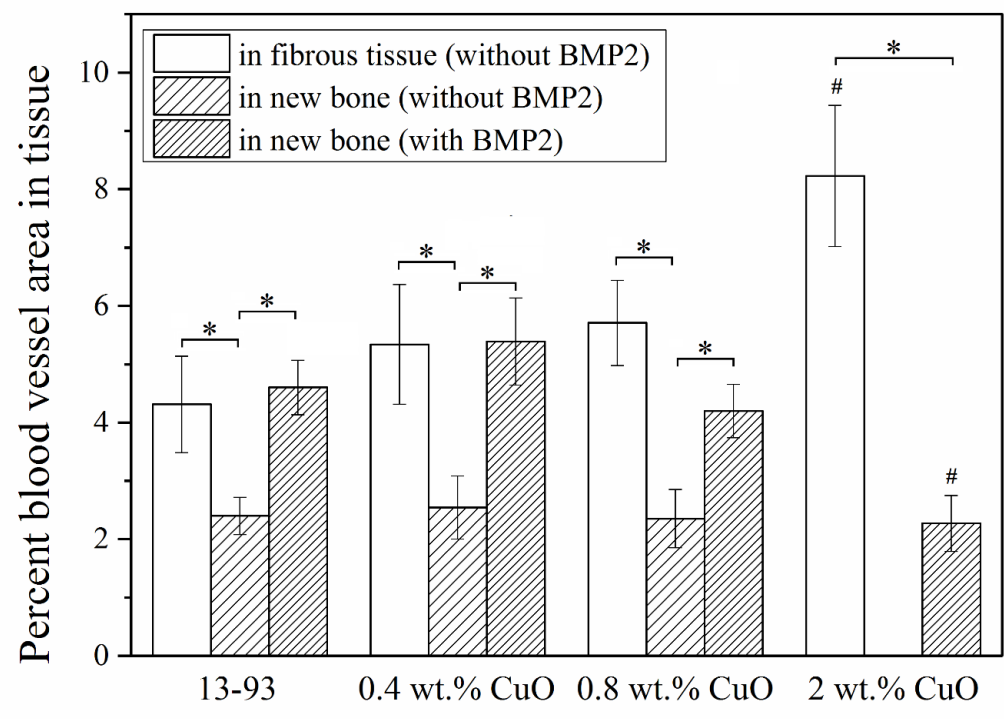


Fig. 13. Percent blood vessel area in rat calvarial defects implanted with the four groups of scaffolds at 6 weeks postimplantation. The blood vessel area in the fibrous tissue and in the new bone are shown (as a percentage of the total fibrous tissue and total new bone, respectively). (*significant difference between groups; #significant difference when compared to 13-93 group; p<0.05)

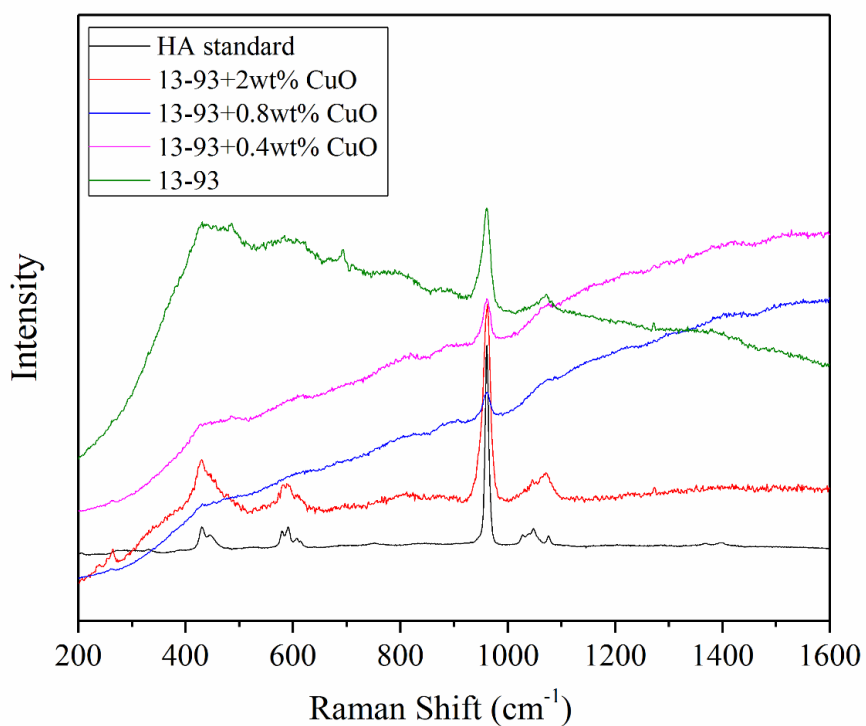


Fig. S1. Raman spectra of the un-doped 13-93 scaffold and the 13-93 bioactive glass scaffolds doped with 0.4 wt.% CuO, 0.8 wt.% CuO and 2 wt.% CuO after immersion in SBF for 28 days. For comparison, the pattern of a reference hydroxyapatite (A027249-1) is also shown.

SECTION

2. CONCLUSIONS

Bone regeneration in rat calvarial defects implanted with strong porous bioactive glass (13-93) scaffolds was studied at implantation times of 12 and 24 weeks and compared with a similar study at 6 weeks. Bone regeneration in the defects implanted with the as-fabricated scaffolds increased significantly with increase in the implantation time from 6 to 24 weeks. Pretreating the scaffolds to convert a thin surface layer to hydroxyapatite enhanced bone regeneration at 6 weeks but not at 12 or 24 weeks. Scaffolds loaded with BMP2 (1 $\mu\text{g}/\text{defect}$) significantly enhanced bone regeneration at all three implantation times. The pore space of the BMP2-loaded scaffolds was almost completely infiltrated with lamellar bone within 12 weeks. The pretreatment or BMP2 loading did not affect the amount of bioactive glass converted to hydroxyapatite at 24 weeks (30%). While blood vessels were present in the new bone that infiltrated all three groups of scaffolds, the BMP2-loaded scaffolds had a significantly higher number of blood vessels and blood vessel area at 6 and 12 weeks post-implantation. Strong porous bioactive glass (13-93) scaffolds loaded with clinically acceptable levels of BMP2 could provide promising implants for healing structural (loaded) bone defects within a clinically relevant time.

Scaffolds with a grid-like microstructure composed of silicate 13-93 bioactive glass doped with varying amounts of Cu (0-2.0 wt. % CuO) were created by robotic deposition and evaluated *in vitro* and *in vivo*. When immersed in simulated body fluid (SBF), the scaffolds released Cu ions in a dose-dependent manner but the Cu doping had no significant effect on the degradation and conversion of the scaffolds to hydroxyapatite. CuO dopant concentrations of 0.4 and 0.8 wt. % had no significant effect on the number and alkaline phosphatase activity of MC3T3-E1 cells cultured on the scaffolds *in vitro* and on bone

regeneration and angiogenesis in rat calvarial defects at 6 weeks postimplantation. CuO dopant concentration of 2.0 wt. % significantly reduced the number and ALP activity of MC3T3-E1 cells *in vitro* and bone regeneration *in vivo* but significantly enhanced blood vessel area in the fibrous tissue that infiltrated the scaffolds. Loading the undoped or Cu-doped scaffolds with BMP2 (1 $\mu\text{g}/\text{defect}$) significantly enhanced their capacity to regenerate bone. Doping 13-93 bioactive glass scaffolds with 0.4 and 0.8 wt. % CuO had no significant effect on the response of MC3T3-E1 cells *in vitro* and bone regeneration in rat calvarial defects *in vivo* but a CuO concentration of 2.0 wt. % was toxic to the MC3T3-E1 cells and severely inhibited bone regeneration.

VITA

Yinan Lin was born on January 4, 1988 in Yantai, Shandong Province, P.R. China. Yinan started his undergraduate education at Shandong University of Technology. With his enthusiasm for biological science, Yinan completed his B.S. degree majoring in Biological Sciences from Shandong University of Technology in July of 2010 and received Outstanding Graduating Student Award of Shandong province. After graduation, he began working on his graduate degree under Dr. Roger Brown at Missouri University of Science and Technology in the Fall of 2010. He received a Master's degree in Biological Sciences from Missouri University of Science and Technology in July 2012.

Driven by his desire for a more fundamental understanding of biomaterials, Yinan started his Master's degree in Materials Science and Engineering in 2012, under the supervision of Dr. Mohamed N. Rahaman at Missouri University of Science and Technology. In December 2015, he received a Master's degree in Material Sciences and Engineering from Missouri University of Science and Technology.